Polarization of atomic ensembles in ionized gases

S. A. Kazantsev, N. Ya. Polynovskaya, L. N. Pyatnitskii, and S. A. Edel'man

Scientific Research Physics Institute, Leningrad State University, and Institute of High Temperatures, Academy of Sciences of the USSR, Moscow

Usp. Fiz. Nauk **156**, 3–46 (September 1988)

Publications devoted to the polarization of the quantum states of ensembles of atomic particles in ionized gases and plasmas are reviewed. A theoretical description of the phenomenon is given and its relationship to anisotropic properties of plasmas is established. Methods of determining the polarization of the states of atomic ensembles from the polarization of the line spectrum of excited particles are described. Experimental studies of gas discharges, beam-plasma systems, and astrophysical objects are summarized. It is shown that the polarization of the quantum states of atoms can be observed over a wide range of plasma conditions.

TABLE OF CONTENTS

1. INTRODUCTION

The polarization of an atomic ensemble is usually understood to be the nonuniform population of the magnetic sublevels of degenerate atomic states or, in other words, an ordering of their angular momenta.[1)] The form of this ordering is described by the so-called *polarization moments* of the atomic density matrix.[1–5] The polarization moment of rank zero (a scalar) is the population of a state, the polarization moment of rank one (orientation vector) determines the mean dipole magnetic moment of the state, and the polarization moment of rank two (alignment tensor) corresponds to the mean quadrupole electric moment. Any particular combination of polarization moments that are necessary for a description of an ensemble of particles depends on the symmetry properties of the processes occurring in the gas and manifests itself in the polarization of the line spectra due to spontaneous emission. For example, an *oriented* ensemble radiates circularly polarized light whereas an *aligned* ensemble emits linearly polarized light.

The following processes that are responsible for the polarization of atomic states are known at present. First, there is anisotropic resonance optical or electronic excitation. The polarization of states by anisotropic optical excitation is due either to a macroscopic anisotropy of the propagation of resonance radiation in the object under investigation, which is due to its limited size in space,[6–8] or, for a particular subensemble, to the Doppler shift of the frequency of moving atoms.[8,9] It is known that states can be aligned in the course of optical self-pumping in plasmas.[10] When electronic excitation is anisotropic, the polarization of the state reflects the spatial symmetry properties of the electron velocity distribution function and is determined for direct processes by the momentum flux tensor of fast electrons.[11–14] It is possible to align atomic states in plasmas during their anisotropic collisional excitation due to the drift motion of heavy particles.[15–18,58,186,187] Moreover, the electric and magnetic fields that are present in the plasma not only affect the particle kinetics, but can also lead to the transformation of its existing polarization of states.[19–21] Consequently, the polarization of an atomic ensemble in plasma is closely related to the presence of special directions within it, i.e., to the structural properties of the plasma and the nonequilibrium associated with them.

This fact, and the advances being made in plasma physics, including new applications of powerful gas lasers, MHD generators, beam-plasma systems, plasmatrons, and studies of the solar atmosphere and other objects in which the structural properties of the medium play a special part, have been

 0038-5670/88/090785-25$01.80

responsible for the recent renewed interest in polarization phenomena. Studies of the polarization of atomic ensembles may also throw further light on charged-particle kinetics in the peripheral regions of classical gas-discharge sources. These regions lie next to the walls and the electrodes, and play a key part in maintaining the plasma, in transferring energy from the external source to the ionized gas, in energy dissipation, and in establishing the charged-particle balance. By virtue of their origin, they exhibit appreciable anisotropy.

Experimental studies of the polarization of atomic ensembles were originally confined to spectroscopy and atomic physics.[7,22–26] The fundamental feature of all these experiments was the use of external sources to control the ordering of the angular momenta, e.g., resonance optical radiation or directional particle beams. Studies of physical effects in ionized gases, due to the polarization of atomic ensembles by external excitation, have unitl now been confined to a number of independent research areas. These include plasma effects in optical orientation,[27] and also polarization phenomena in plasmas interacting resonantly with a laser field.[28]

The history of the polarization of excited states of particles by internal processes in plasmas has its origin in the 1920s, following the first indications that such phenomena were possible.[29] Partial intrinsic linear polarization of radiation emitted by ionized gases was subsequently observed in astrophysical objects in which these phenomena provided the basis for remote determinations of certain local parameters.[6,30–32]

Further work on the polarization of particle states in plasmas was stimulated by the creation of the necessary mathematical formalism such as the irreducible representations of the atomic density matrix, by various advances in coherent laser spectroscopy and polarimetry, and by studies of plasma-particle kinetics and of the cross sections for elementary processes participating in the ordering of the particle angular momenta.

Studies of the polarization of atomic ensembles in plasmas have now reached a mature stage and our review is the first attempt at a summary of the subject. We shall consider the fundamentals of the theoretical description of the polarization of quantum mechanical states of an ensemble of excited particles in terms of the atomic density matrix, and will present a general approach to the description of the electron kinetics and of the polarization of an ensemble of atomic particles in plasmas. We shall also analyze the characteristic features of the kinetics of the polarization moments under a wide range of external conditions. We shall discuss experimental arrangements for observing the polarization effects in plasmas, including polarimetric methods and methods based on the Hanle effect (the magnetooptical method). We shall use all this as a basis for analyzing experimental data provided by polarization studies and leading to the following conclusion. The polarization of particle states exists under the same conditions as the ionized gas, i.e., in the presence of electric and magnetic fields, directed radiation and particle fluxes, and limitation in space. Consequently, as long as the ionized state exists, the particle ensemble will be polarized. The degree of this polarization can be different, and special techniques as well as high experimental precision are sometimes necessary to detect it. Nevertheless, the phenomenon has been observed in a wide range of objects, including the positive column of the glow discharge,[33,34] the high-frequency[35,36,115] and beam-plasma discharges,[37] the hollow-cathode discharge,[38,39] the Knudsen discharge,[40] the high-voltage diode,[41] the low-pressure[29] and atmospheric-pressure[13,42] arc discharges, the plasmas produced by a relativistic electron beam entering a neutral gas,[43] and so on. There are reasons for concluding that the phenomenon occurs in the working plasma of the MHD generator[44] and in the polar aurora.[45]

These experiments have already identified a number of interesting features in the behavior of plasmas, including electron kinetics, energy transfer, and so on. They serve as the starting point for the development of contractless methods of determining the local parameters of anisotropic plasmas. The theoretical treatment of the polarization of atomic states that has been developed enables us to reinterpret existing experimental data and to achieve a deeper understanding of physical processes in ionized gases.

2. THEORETICAL DESCRIPTION OF THE POLARIZATION OF AN ENSEMBLE OF EXCITED PARTICLES

2.1. Polarization moments of the atomic density matrix

When radiation emitted by an ionized gas is observed, the ensemble of atoms that is involved in the process constitutes a statistical mixture of states. The most general description of this ensemble is provided by the density matrix $\hat{\rho}$ (see, for example, Refs. 46 and 47) which is a generalization of the distribution function of classical mechanics.

In quantum mechanics, the entire information about the behavior of a given system can be expressed in terms of the expectation (average) values of suitably chosen operators. Since the expectation values of a quantity A can be obtained by means of the operation $\mathrm{Tr}(\hat{\rho}\hat{A})$, the density matrix contains the entire physically significant information about the system. Special cases are best treated by taking the representation of the density matrix that best reflects the physical properties of the problem and simplifies the calculations. When it is desirable to exploit the angular symmetry of the ensemble, the density matrix $\hat{\rho}$ can be expanded in terms of the orthogonal irreducible tensor operators $\hat{T}$ (Refs. 48 and 49).

The systematic use of tensor operators was first suggested by Fano.[2] It has since been extensively used in the theory of angular correlations in nuclear physics,[50] in atomic physics,[3,5,25,51] in research into optical pumping,[452] in experiments on quantum beats,[47] and in experiments with atoms excited by laser radiation.[7,53,54]

The expansion of $\hat{\rho}$ in terms of the irreducible basis is

$$\hat{\rho} = \sum_{\alpha\alpha', JJ', \varkappa q} \rho_q^{(\varkappa)}(\alpha J,\ \alpha' J')\, \hat{T}_q^{(\varkappa)}(\alpha J,\ \alpha' J'), \qquad (2.1)$$

where J is the total angular momentum of the state, α represents all the remaining quantum numbers that define the state of the ensemble, $T_q^{\varkappa}$ is a tensor operator of rank $\varkappa$, and $|J-J'| \leqslant \varkappa \leqslant J+J'$, $-\varkappa \leqslant q \leqslant \varkappa$.[55]

The diagonal elements $\rho_q^{(\varkappa)}(\alpha J, \alpha J)$, are often referred to as the polarization moments and have a clear physical interpretation. The quantity $\rho_0^{(0)}$ is simply the normalizing constant proportional to the total population of the state $\{\alpha J\}$. The three components of the tensor with $\varkappa = 1$ and $q = 0, \pm 1$ transform as the component of a vector frequently referred to as the *orientation vector*. If we use (2.1) together with the orthogonality condition of $\rho_q^{(\varkappa)}$, we can show that

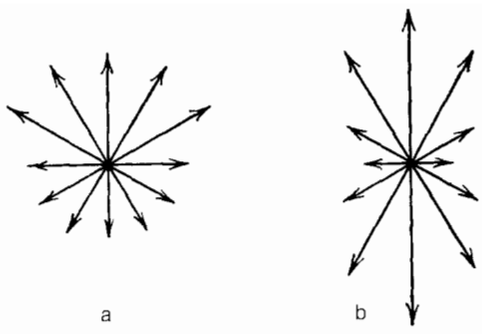

FIG. 1. Spatial distribution of angular momentum vectors typical for oriented (a) and aligned (b) systems of excited particles.

the orientation vector is proportional to the total magnetic dipole moment of the system. The tensor $\rho^{(2)}$ is called the *alignment tensor* and determines the electric quadrupole moment of the ensemble.[47]

In ionized gases, the symmetry of the system under investigation is usually determined by fields acting within it, or by fluxes of radiation and of particles. The simplest and the most commonly encountered are axially-symmetric systems in which there is one special direction. General laws of symmetry then demand that the aligned ensemble of particles is the only one that can be formed.

The physical picture of the phenomenon can be clearly presented as follows.[47] When $q = 0$, there are only the diagonal components ρ_{MM} of the density matrix in the JM representation, i.e., the state is completely described by the distribution of populations over the magnetic sublevels. In the semiclassical picture, a vector of length $\{JM\}$ that precesses around the z axis is associated with the state $[J(J+1)]^{1/2}$, and its z-component is equal to M. The length of the vector can be altered, without altering its direction in space, in such a way that it becomes proportional to the number of particles in the corresponding state $\{JM\}$. If we start with this model, the aligned system can be represented by the diagram of Fig. 1 in which arrows represent the angular momentum vectors and have certain allowed directions in space. The diagram is axially symmetric and invariant under the operation $z \to -z$, i.e., vectors that have opposite directions have equal lengths. The diagram thus shows that the total angular momentum $\langle \hat{J} \rangle$ of an aligned system is zero. In the absence of invariance under space inversion, the states $\{JM\}$ and $\{J-M\}$ have different populations, and we can have, for example, the oriented system whose diagram is also shown in Fig. 1. It is clear that, in this case, there is a nonzero total angular momentum $\langle \hat{J} \rangle$ pointing along the z axis. The oriented ensemble can arise, for example, when atoms are excited by circularly polarized light. The polarization moments of the density matrix $\rho_q^{(\varkappa)}$ are directly related to the polarization characteristics of the radiation emitted by an ensemble of atoms as a result of electric dipole transitions. In the most general form, the polarization of radiation is described by the Stokes parameters η_0, η_1, η_2, η_3, η_0 that determine the total intensity of radiation propagating in a particular direction and depend on population $\rho_0^{(0)}$ and alignment $\rho_q^{(2)}$. The Stokes parameter η_1 is the difference between radiation intensities that are linearly polarized along mutually perpendicular axes, and is proportional to the degree of linear polarization P. The parameter η_2 is defined in the same way as η_1 except that it is referred to axes rotated through 45° to the direction of the original axes.

The parameters η_1 and η_2 depend only on $\rho_q^{(2)}$, i.e., on the mean electric quadrupole moment of the ensemble of radiating particles. The quantity η_3 corresponds to the intensity difference between radiation components with right- and left-handed circular polarizations, and is proportional to the component $\rho^{(1)}$ of the orientation vector along the chosen direction of observation.

Thus, dipole radiation cannot have a polarization moment of rank higher than two. Higher-order moments can be observed in forbidden transitions[56] or in interactions between atomic systems and strong resonant fields.[28,57]

2.2 Elementary polarization processes in an atomic ensemble

The polarization of an atomic ensemble can be due either to excitation or relaxation processes. In plasmas, excitation is most frequently due to resonance radiation and to collisions with electrons.

We begin by considering the effect of resonance radiation. In general, the intensity of incident radiation can be expanded in the dipole approximation in terms of spherical harmonics, as follows:

$$I(\mathbf{k}) = \frac{2\pi}{\hbar} u (2J_a+1)^{-1} \sum_{\varkappa=0}^{\infty} \sum_{q=-\varkappa}^{\varkappa} (-1)^{J_a+J_b+\varkappa+1} \times \begin{Bmatrix} J_b & J_b & \varkappa \\ 1 & 1 & J_a \end{Bmatrix} \Phi_q^{(\varkappa)}(\varepsilon)\, Y_q^{(\varkappa)}(\theta, \varphi), \tag{2.2}$$

where $\Phi_q^{(\varkappa)}(\varepsilon)$ is the observation tensor defined in Ref. 25 and u is the radiation flux density. The polarization moments $\rho_q^{(\varkappa)}$ that arise as a result of photoabsorption are proportional to the corresponding intensity multipoles $I_q^{(\varkappa)}$ that reflect the geometric and polarization properties of the resonant optical emission of plasmas. This relationship is indicated by a number of laboratory experiments and by astrophysical observations.[30,31,60,61]

Electron impact, especially in the region of threshold energies, has much in common with excitation by linearly polarized resonance radiation.[62] The main assumption that is usually made when an elementary excitation event is considered follows from the Persival-Seaton hypothesis[63] and consists of neglecting all spin-dependent forces during the collision time. The significance of this is as follows.

In the excited state, the orbital angular momentum L and the spin angular momentum S are coupled by the fine interaction and precess around the common angular momentum J. The characteristic procession time is $\tau_{LS} \sim \hbar/\mathscr{E}_{LS}$ where $\mathscr{E}_{LS}$ is the fine splitting energy. If the collision time ($\tau_c \sim 10^{-15}$ s) is much shorter than the precession period, the orbital angular momentum and the spin angular momentum can be looked upon as uncoupled during the collision period. The state of an excited atom after the collision can be satisfactorily described by the LS-coupling scheme. The inequality $\tau_c \ll \tau_{LS}$ implies that the atoms are excited instantaneously and serves, at the same time, as a measure of the validity of this approximation.[64-67]

When atoms are excited by a collimated monoenergetic beam of electrons, the elements of the density matrix averaged over all spins are given by[47]

$$\rho_q^{(\varkappa)}(L) = \sum_{M, M'} (-1)^{L-M'} C^{\varkappa q}_{LM'L-M} \rho_{LM, LM'}, \tag{2.3}$$

where $C^{\varkappa q}_{LM\,L-M}$ is the Clebsh-Gordan coefficient.

The collision geometry has cylindrical symmetry in the case of averaging over scattered electrons. Consequently, the properties of the excited atomic ensemble are invariant under rotations around this axis, so that all moments with $q \neq 0$ must vanish. The polarization of states then reduces to the nonequilibrium population of magnetic sublevels, where $\rho_{LM,\,LM} = \rho_{L-M,\,L-M}$ and $\rho_0^{(\varkappa)}$ with odd $\varkappa$ are zero, and the dipole radiation reflects only the population and the longitudinal alignment $\rho_0^{(2)}$.

It is often more convenient to use the cross sections for the excitation of the corresponding polarization moments. Let Q_M represent the cross section for the excitation of a sublevel M. We then have

$$\begin{aligned} \rho_0^{(0)} &= N_e v \rho_0^{(0)}(g)\, Q^{(0)} \Gamma^{-1} (2L+1)^{-1/2}, \qquad Q^{(0)} = \sum_M Q_M, \\ \rho_0^{(2)} &= N_e v \rho_0^{(0)}(g)\, \Gamma^{-1} \sum_M (-1)^{L-M} C^{20}_{LML-M} Q_M, \end{aligned} \tag{2.4}$$

where $\rho_0^{(0)}(g)$ is the population of the ground state, Γ is the probability of the radiative decay of the excited state, and N_e is the electron concentration. The quantity

$$Q^{(2)} = \sum_M (-1)^{L-M} C^{20}_{LML-M} Q_M \tag{2.5}$$

then has the meaning of the cross section for the excitation of alignment.

Let us examine how this cross section varies with electron energy. For threshold excitation, the incident electron cannot transfer angular momentum to the atom and the only transitions are those between sublevels with the same value of M. When the lowest state has angular momentum $L = 0$, the only sublevel to be excited is that with $M = 0$. As the electron energy increases, sublevels with $M \neq 0$ begin to be populated. At energies much greater than the threshold energy $\mathscr{E}_t$, the Born approximation becomes valid and the collision can be looked upon as a fast transfer of momentum $\mathbf{K}_e = \mathbf{k}_e - \mathbf{k}'_e$ where $\mathbf{k}_e$ and $\mathbf{k}'_e$ are the wave vectors of the incident and scattered electrons, respectively (see Fig. 2). The vector $\mathbf{K}_e$ is then the only parameter that governs the character of the population of magnetic sublevels of the excited state. In the coordinate frame in which the z axis is parallel to $\mathbf{K}_e$, the electron cannot transfer to the atom any angular momentum along the z axis, and only a population and a longitudinal alignment $\rho_0^{(2)}(\mathbf{K}_e)$ can be produced in $\mathbf{K}_e$ system. Rotation of the alignment tensor from the $\mathbf{K}_e$ system to the laboratory system gives

$$Q^{(2)} = -\frac{1}{2} Q^{(2)}(\mathbf{K}_e)(1 - 3\cos^2\psi), \tag{2.6}$$

where ψ is the angle between the vectors $\mathbf{K}_e$ and $\mathbf{k}_e$. At the same time,

$$Q^{(0)} = Q^{(0)}(\mathbf{K}_e), \qquad Q^{(2)}(\mathbf{K}_e) = \frac{C^{20}_{L0L0}}{C^{00}_{L0L0}} Q^{(0)}.$$

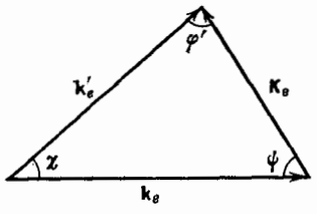

FIG. 2. Wave vector triangle for the collision of an electron with an atom.

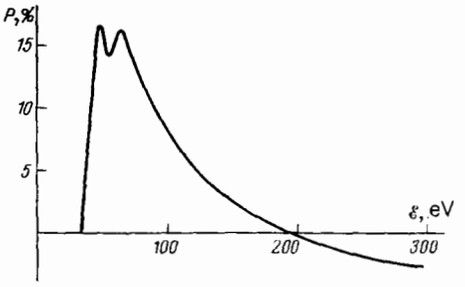

FIG. 3. Polarization of the 492.2-nm line of helium as a function of the energy of the exciting electrons.[68] Gas pressure 0.011 torr, electron beam current 2.5 mA.

If we average (2.6) over all the possible values of the angle ψ, we obtain

$$\tilde{Q}^{(2)} = \frac{Q^{(2)}}{Q^{(0)}} = -\frac{1}{2} \frac{C^{20}_{L0L0}}{C^{00}_{L0L0}} (1 - 3\langle\cos^2\psi\rangle). \tag{2.7}$$

At the excitation threshold, we have $\psi = 0$. Small-angle scattering predominates at energies $\mathscr{E} \gg \mathscr{E}_t$, and momentum is transferred at right angles to the direction of the electron beam. Consequently, the ratio $\tilde{Q}^{(2)}$ is a maximum near the threshold, but then falls to zero, changes sign, and at high electron energies its absolute magnitude tends to half its threshold value. The degree of polarization of the radiation behaves in a similar way. As an example, Fig. 3 shows the function $P(\mathscr{E})$ for the HeI line with $\lambda = 4922$ Å (Ref. 68). The expressions for $\langle\cos^2\psi\rangle$ for allowed and forbidden transitions are derived in Refs. 70 and 71 in terms of the *alignment parameter* $A \sim Q^{(2)}$ (Ref. 69).

The values of $Q^{(0)}$ are usually obtained in one of two possible experiments, namely, experiments with crossed particle beams, or experiments with an electron beam injected into a homogeneous gas. In both cases, the fluorescence intensity due to excited particles is proportional to $Q^{(0)}$. In some of these experiments, measurements are also made of the polarization of the radiation, so that $Q^{(2)}$ can be found. This subject is reviewed in Refs. 72 and 73.

Let us now briefly consider the role of relaxation phenomena in the polarization of atomic ensembles. The number of processes responsible for the relaxation of excited states in plasmas is relatively large. They include spontaneous emission, collisions between particles, radiation trapping, the effects of stochastic plasma fields and weak external electric and magnetic fields, and so on. Most of them have a high degree of symmetry, are frequently isotropic, and cannot lead to the formation of polarized states (they simply reduce existing polarizations). Actually, in an isotropic system, the relaxation matrix performs a scalar transformation and does not alter $\varkappa$ or q, i.e.,

$$\Gamma^{\varkappa\varkappa'}_{qq'} = \gamma_\varkappa \delta_{\varkappa\varkappa'} \delta_{qq'}.$$

However, in many cases, e.g., in the presence of drifting ions whose energy is insufficient for the direct excitation of atomic states, the relaxation process is anisotropic.

The transport equations for the simultaneous relaxation of polarization moments with $q = 0$ are used in Refs. 74 and 75 as a basis for an analysis of the possibility of alignment of narrow atomic ^{2}P doublets under the influence of drifting ions. Estimates show that, in low-pressure plasmas, the drift of ions under significantly nonequilibrium condi-

tions will probably compete with other alignment mechanisms because of the high cross section for the process (10^{-12}–10^{-11} cm^2 for ion velocities $v \sim 10^5$ cm/s). The same process can be considered from another point of view.[17] In the coordinate frame moving together with the beam, the ions are in a stream of neutral particles that is antiparallel to the ion drift. Consequently, the ions also experience the effect of anisotropic collisions which, in accordance with the foregoing, should lead to a longitudinal alignment of their narrow multiplets. The theoretical prediction of the drift mechanism of alignment of ions has been confirmed experimentally by studies of the polarization of the line spectrum of hollow-cathode discharges.[18,186,187]

When an ensemble of atoms experiences not only anisotropic collisional relaxation, but also a weak constant magnetic field that is perpendicular to the ion beam axis, it exhibits a further interesting phenomenon, namely, the transformation of longitudinal alignment into *transverse orientation*.[21]

The transformation of alignment into orientation is also found to occur under typical conditions under which the alignment of atomic states is investigated experimentally in a dc gas discharge using the Hanle method, since the method itself relies on the application of a weak magnetic field (see Section 4.2).

In addition to the above mechanism, the $\rho^{(2)} \to \rho^{(1)}$ transition can also occur in a weak magnetic field during the excitation of atoms by electron impact,[20] the recoiling of atoms during their excitation by high energy ions,[76] the nonlinear interaction of atoms with an exciting light field that is frequency-shifted relative to the center of the atomic spectral line,[77] or during the interaction between atoms and coherent resonance radiation.[77,78] The role of each of these mechanisms depends significantly on the particular physical conditions.

3. ANISOTROPY IN THE MOTION OF ELECTRONS AND THE POLARIZATION KINETICS OF ATOMIC ENSEMBLES

3.1. Multipole expansion of the electron distribution function

The polarization of atomic ensembles in plasmas is due to anisotropic processes which, in particular, may be due to a departure from equilibrium. The electron distribution function (EDF) is particularly sensitive to external effects. It may therefore be significantly different from the equilibrium function, but the heavy-particle distributions are often nearly Maxwellian.[80] Even for moderate values of E/p, the electron temperature may be significantly different from the temperature of the atoms and the EDF may acquire anisotropic properties, especially at high energies ($\mathscr{E} > T_e$). As a result, excitation by electrons is often the main mechanism responsible for the polarization of states.

The particular feature of electronic excitation of atomic ensembles in plasmas, as compared with the classical beam experiments discussed in Section 2.2, is the difference between the angular and velocity EDF and the δ-function. This is why, in the present context, the properties of the polarization of states present themselves in a masked form. To understand them, it is essential to have a convenient method of classifying order in the motion of electrons. This can be done by expanding the electron distribution function in terms of an irreducible basis. As in the case of the atomic density matrix, this enables us to separate the angular part of the EDF from the energy part. This basis is usually taken in the form of the spherical functions $Y_q^{(\varkappa)}$:

$$f(\mathbf{v}, \mathbf{r}, t) = \sum_{\varkappa, q} f_q^{(\varkappa)}(v, \mathbf{r}, t) Y_q^{(\varkappa)}(\theta, \varphi), \tag{3.1}$$

where $\mathbf{r}$ is the radius vector and θ, φ are angles defining the direction of the velocity vector $\mathbf{v}$. The expansion coefficients $f_q^{(\varkappa)}$ are the multipole moments of the EDF, and have a clear physical meaning: the zero-order moment $f_0^{(0)}$ is a measure of the number of particles per unit volume, the first moment $f_q^{(1)}$ determines the velocity vector, the tensor $f_q^{(2)}$ determines the anisotropic pressure or momentum flux tensor, and $f_q^{(3)}$ is the energy flux tensor.

Since these spherical functions (harmonics) are orthogonal, the moment of the density matrix of rank $\varkappa$, produced under direct excitation by electrons with a distribution function of the form given by (3.1), is determined by the expansion coefficient $f_q^{(\varkappa)}$ (Ref. 11):

$$\rho_q^{(\varkappa)} = N_e \rho_0^{(0)}(g)\, \Gamma^{-1} \int_0^\infty v^3 f_q^{(\varkappa)}(v)\, Q^{(\varkappa)}(v)\, dv. \tag{3.2}$$

In particular, the source of alignment of excited atoms and, hence, of the linear polarization of the emitted radiation, can only be the electron momentum tensor.

Expansion of the EDF in terms of spherical harmonics (more frequently, in terms of the Lagrange polynomials $P_\varkappa(\cos\theta) = Y_0^{(\varkappa)}(0, \varphi)$) is a standard technique in physics. However, as a rule, such calculations are usually confined to the first two terms of the expansion, $f^{(0)}$ and $f^{(1)}$, which are used to find the electron concentration and the transport coefficients (conductivity of the medium, diffusion coefficient, thermal conductivity, and so on). The use of the two-term approximation implies that the distribution function is weakly anisotropic, at least no more than $\cos\theta$. Recent publications have analyzed the validity of this approximation and have noted that the presence of parameter gradients,[42,81] electric-field gradients,[81–89] and discontinuities in potentials,[40,145,188] can complicate the symmetry properties of the EDF and ensure that the higher-order moments become significant, so that the Boltzmann equation may have to be modified.[81] The convergence of the series given by (3.1) must then be analyzed, and the role of each of the harmonics elucidated. However, it is important to emphasize once again that it is the second moment of the EDF that is responsible for the alignment of excited particles and the linear polarization of their emission. Knowledge of the polarization of an atomic ensemble is thus seen to offer us the basic possibility of obtaining extensive information on plasma parameters, namely, the spatial distribution of the anisotropy of the local electron distribution function and, consequently, energy losses, instabilities, electric and magnetic fields, and so on.

3.2. Anisotropic characteristics of the electron distribution function in an electric field

We must now consider in greater detail the symmetry properties of the electron distribution function in a plasma located in an external electric field. We shall consider three aspects of the problem, namely, alternating electric field, anisotropy in the scattering of electrons by heavy particles, and radial parameter gradients in collisional plasma.

The Boltzmann equation has been solved in the form of

an expansion in terms of the Legendre polynomials[90] for the case of an alternating electric field. The analysis was performed for a spatially homogeneous plasma, subject to the condition that the multipole moments of the distribution function of rank higher than 2 could be regarded as small.[12] When

$$f_0^{(0)} \sim \exp\left(-\frac{mv^2}{T_e}\right),$$

then for electron energies

$$\mathscr{E} > m_e T_e^2 \frac{\nu_{ea}^2 + \omega_0^2}{2(eE)^2}$$

the motion of the electrons exhibits appreciable anisotropy that is determined mostly by the second moment of the EDF (ν_{ea} is the electron-atom collision frequency and ω_0 is the frequency of the HF field). These estimates have been confirmed experimentally and were used in Ref. 91 to determine the HF field by the methods of polarization spectroscopy.

The influence of anisotropy in the scattering of electrons by heavy particles on the angular properties of the EDF was investigated in Ref. 88 in the following simplified model:

—no energy transfer in collisions between electrons and the gas

—scattering occurs only at 0° and 180°

—the velocity dependence of the total cross section has the form $v^p (p \sim 1-2)$.

It is found in this approximation that, at low energies, electron scattering occurs with practically the same probability in all directions and, hence, after the collision, the electron again speeds up in the direction of the field. Small-angle scattering predominates at high energies, i.e., the velocity of the electron after the collision has only a slightly different direction, and the electron continues to speed up in the direction of the field. This means that anisotropic scattering may be an efficient mechanism for producing *runaway* electrons. Moreover, it can influence the reaction rate constants and the transport coefficients of plasmas. It has been shown[83,85] that the maximum changes in the diffusion coefficients occur for high average inelastic collision frequencies, e.g., when the ratio of elastic to inelastic cross sections approaches unity. Thus, even when the electron drift velocity is appreciably lower than the thermal velocity, this cannot be regarded as sufficient grounds for neglecting the terms with $\varkappa > 1$ in (3.1). A similar conclusion is reported in Refs. 93 and 94.

An analogous investigation, using realistic collision cross sections, was performed in Ref. 87, where, in the course of the solution of the Boltzmann equation, the collision cross sections were determined in terms of the differential scattering cross sections $\sigma(\chi, \mathscr{E})$:

$$\sigma_\varkappa(\mathscr{E}) = 2\pi \int_0^\pi \sigma(\chi, \mathscr{E}) P_\varkappa(\cos\chi) \sin\chi \, d\chi. \qquad (3.3)$$

The cross sections $\sigma(\chi, \mathscr{E})$ were taken from the extensive published experimental and theoretical data[93–99] on the nitrogen molecule. Six terms in the expansion in terms of the Legendre polynomials were taken into account. Comparison with experiment showed that, for most of the transport coefficients and reaction rates, it was more important to take into account the higher-order multipole moments of the EDF than the anisotropy of the scattering process, but both factors had to be allowed for in exact analysis. The effect was particularly noticeable for high values of the ratio E/p and high electron energies.

Apart from external electric fields, plasma-parameter gradients, e.g., in boundary layers, can give rise to anisotropy in the motion of electrons. The combined effect of a radial parameter gradient and an axial constant electric field was discussed in Ref. 42 for axially-symmetric plasmas. Analytic solutions of the Boltzmann equation were obtained, using the first five terms of the multipole-moment representation, and it was shown that, if the multipole moments of the EDF decrease rapidly with increasing rank of the moment at low electron energies (i.e., the distribution of thermal and subthermal electrons is practically isotropic), the higher-rank moments may actually exceed the first moment in the tail of the distribution function.

Figure 4 shows graphs of $f_q^{(2)}(\mathscr{E})$ as a function of $\mathscr{E}$ for a number of values of the radial coordinte R and plasma parameters corresponding to an arc discharge in argon at atmospheric pressure ($T_e \sim 1$ eV, $N_e \sim 10^{17}$ cm^{-3}). It is clear from the figure that the maxima of these curves are shifted relative to the thermal energy, and occur at $\mathscr{E} \sim 5$–6 eV. At the same time, the thermal and subthermal electrons are virtually isotropic. The anisotropy in the motion of fast electrons is determined by the accelerating external field and the gradients of T_e and N_e. The result of this is that, in the axial region of the plasma, in which the radial derivatives of T_e and N_e are zero, the tensors $f_q^{(\varkappa)}$ have only the single $q = 0$ component. All the components of $f_q^{(\varkappa)}$ appear as the

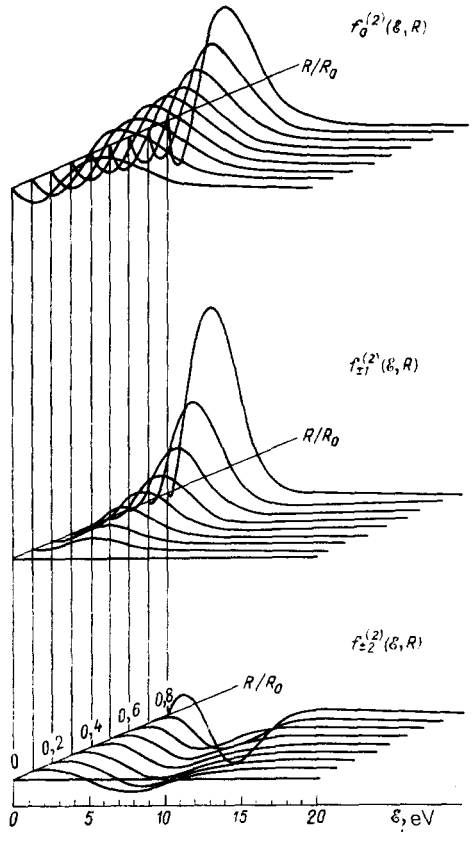

FIG. 4. Radial and energy profiles of the components of the tensor $f^{(2)}$ (Ref. 42).

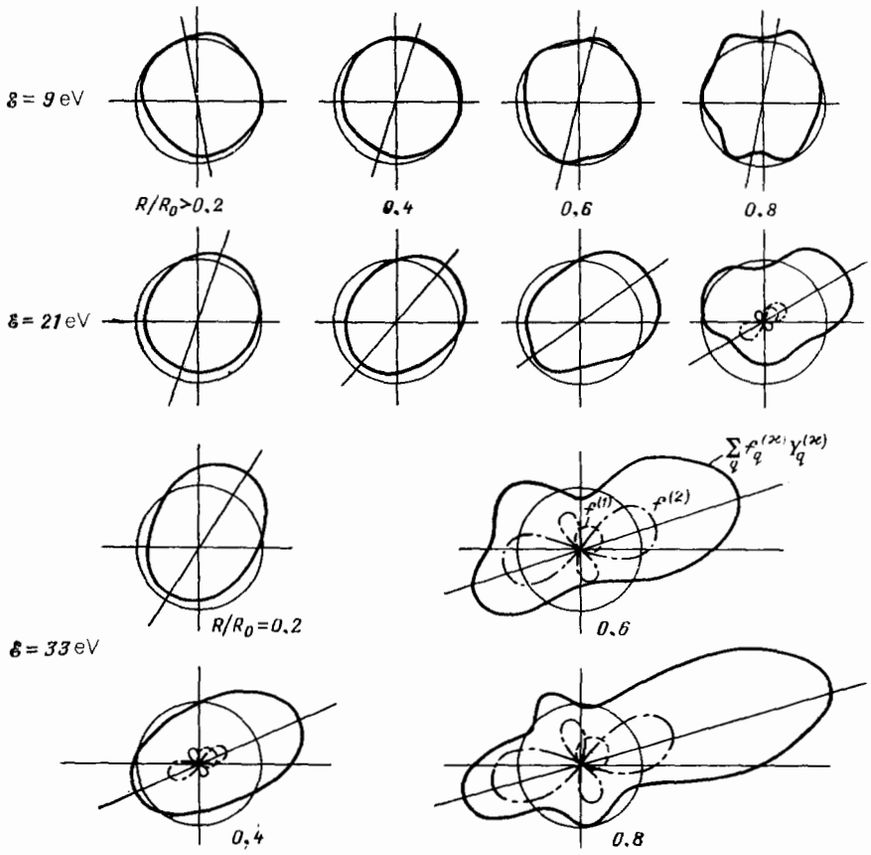

FIG. 5. Angular distribution functions of electrons in an arc discharge.[42]

distance from the axis increases, and each tensor acquires two principal axes. We shall demonstrate this by considering the example of the momentum flux tensor $f^{(2)}$. It will be sufficient to rotate the original coordinate frame through the angle

$$\theta = \frac{1}{2}\operatorname{arctg}\frac{2f_1^{(2)}}{\sqrt{3/2}\,f_0^{(2)} - f_2^{(2)}}.$$

In the new coordinate frame, the components $f_{\pm 1}^{(2)'}$ are zero, but the components $f_{\pm 1}^{(2)'}$, which characterize the anisotropy in the direction at right angles to the z axis, have nonzero values, as before. Physically, this reflects the different nature of the directed motion of electrons in the axial and radial directions, and shows that there are two mutually perpendicular and independent quasibeams of electrons.

We now turn to Fig. 5 which shows in terms of polar coordinates the total electron distribution function (3.1), normalized to the zero-rank moment, for three values of the energy ($\mathscr{E} = 9$, 21, and 33 eV) and four values of the radial coordinate ($R/R_0 = 0.2$, 0.4, 0.6, and 0.8). It is clear that, when $R \sim 0$ the main distortion of the EDF occurs in the axial direction, and a deficit of fast electrons is observed at large angles θ and is due to the external electric field. Near the plasma boundary, the direction of the anisotropy in the distribution function is at an angle of $\theta = 70$–$80°$ to the axis of the discharge, which has a particularly strong effect on the motion of high-energy electrons. It is clear that this is due to parameter gradients (especially temperature gradients). The role of the different moments varies with increasing distance from the axis and increasing electron energy. When $\mathscr{E} = 9$ eV, we have $f^{(0)} \gg f^{(1)}, f^{(2)}$ (and $f^{(1)} > f^{(2)}$); at 21 eV, the departure of the EDF from the isotropic function is very appreciable and is determined mostly by the second-rank moment $f^{(2)}$, i.e., the momentum flux and not the directed velocity $f^{(1)}$. When $\mathscr{E} = 33$ eV, the distortion of the distribution function is so large that $f^{(2)}$ begins to exceed $f^{(0)}$, whereas $f^{(1)}$ increases only slightly. Moreover, at the extreme point considered in these calculations ($R/R_0 = 0.8$), all the high-rank moments up to $\varkappa = 4$ increase with increasing rank, and there are reasons to suppose that the series given by (3.1) begins to diverge.[2)]

Apart from the convergence of the series, this raises the question of the *locality* of the distribution function and of other possible reasons for the modification of the Boltzmann equation. However, these complications are not of practical importance because the number of carriers of energy $\mathscr{E} \gg T_e$ is small. Actually, calculations show that, for the conditions corresponding to Fig. 4, the density of electrons with $\mathscr{E} \gtrsim 30$ eV on the boundary of plasma ($R/R_0 = 0.8$; $N_e \approx (0.4 \times 10^{17}\ \text{cm}^{-3}$, $T_e = 1.11 \times 10^4$ K) is about 300 cm^{-3}. A distribution function of this kind exists on paper only, and the beam of electrons may be replaced by occasional electron bursts. The question of the convergence of the series and of the modified Boltzmann equation then becomes meaningless. On the other hand, under the other conditions of this example, inclusion of the second moment $f^{(2)}$ ensures that the process will be described with sufficient precision. Of course, there may be some special experimental situations in which it will be essential to include higher-rank moments, or even improve the Boltzmann equation.

Summarizing the above discussion, we conclude that electrons with energies $\mathscr{E} = 10$–20 eV will participate in the polarization of an ensemble of atoms, since at lower energies

the anisotropy of the EDF ($f^{(2)}$) is small, whereas at high energies the number of electrons is small. We now turn to the analysis of polarization processes in the presence of anisotropic excitations.

3.3. Kinetics of polarization moments in plasmas

The fact that, for electrons with energies close to the threshold for inelastic processes, the distribution function is anisotropic, is actually valid for a wide range of objects. It is natural to expect that, by virtue of (3.2), electronic excitation can lead to the alignment of particle states in plasmas. However, as already noted, (3.2) is valid only for direct excitation processes that, in reality, are not the only ones by far. Hence, just as the adequate interpretation of spectroscopic data demands a knowledge of the population kinetics of the particle states, so an understanding of polarization phenomena relies on the availability of the appropriate information on the kinetics of anisotropic excitation and relaxation.

The simplest and the most extensively investigated is the alignment kinetics of states in low-pressure plasmas,[7,31] where direct electron impact has a major significance in the excitation of atoms.[80] The same process may be responsible for the alignment of atoms in the case of an anisotropic electron distribution function. Population relaxation, determined by radiative transitions, is then accompanied by the transfer of alignment to lower-lying states. Moreover, alignment will be disturbed by ground-state atoms as a result of collisions leading to transitions to magnetic sublevels of a given state $\{\alpha J\}$, i.e., the so-called depolarizing collisions.

The situation is complicated by radiation trapping. This can play a twofold role. First, radiation trapping leads to an increase in the effective photon lifetime within the plasma. The result of this is a reduction in the rate of decay of excited states, which becomes difficult for each moment of the density matrix, and is always smaller than the reciprocal of the natural lifetime.[3] Because the light flux in a bounded plasma is anisotropic, radiation trapping may also be a source of the polarization of states. Of course, the alignment tensor will then have the same symmetry as the angular distribution of radiation intensity. Optical alignment in plasmas has been extensively investigated and has been discussed in a number of reviews and monographs.[7,59,60,100] We shall not, therefore, discuss it in detail here.

The stationary alignment of a state i in the observationally most favorable situation, in which there are no cascade transitions to the given state from higher-lying levels, no trapping of radiation, and no external fields, can be calculated from the formula

$$\frac{\rho^{(2)}}{\rho^{(0)}}=\frac{F_{gi}^{(2)}/F_{gi}^{(0)}}{1+[\gamma_2/(\Gamma+\gamma_0)]}, \tag{3.4}$$

where

$$\Gamma=\sum_{j<i}A_{ij}, \quad \gamma_0=N_a\langle\sigma_0 v\rangle, \quad \gamma_2=N_a\langle\sigma_2 v\rangle,$$

F_{gi} is the alignment excitation function for the state i from the ground state, N_a is the concentration of atoms in the ground state, and σ_0 and σ_2 are the quenching and depolarization cross sections, respectively.

In tenuous plasma, the lifetime of a state depends mostly on radiative processes, and $\gamma_0 \ll \Gamma$. Since the ratio γ_2/Γ increases with increasing pressure (it may reach 10 at pressures of a few torr), the degree of polarization decreases rapidly. This explains why the possibility of observing polarization phenomena in denser media has been regarded with a degree of skepticism. However, it follows from (3.4) that, as the pressure increases, not only γ_2, but also γ_0, are found to increase, and, when γ_2 becomes comparable with Γ, the ratio $\gamma_2/(\Gamma+\gamma_0)$ may not be too high. This can be explained on the basis of simple physical considerations. In media at high enough pressure, $\gamma_0 \gg \Gamma$ and the relaxation of excited states is due to quenching collisions. Since quenching and radiative decay are statistical processes, and since probabilities for such media are multiplied together, the probability of emission is given by the product of the probability of the absence of quenching in time t and the probability of radiative decay, calculated on the assumption that quenching has not taken place, i.e.,

$$P_{rad}=e^{-\gamma_0 t}(1-e^{-\Gamma t}).$$

This expression has a maximum at the point

$$t_{rad}=\Gamma^{-1}\ln\left(1+\frac{\Gamma}{\gamma_0}\right)\approx\gamma_0^{-1},$$

so that the characteristic time at which emission occurs is determined by quenching. Like depolarization, quenching is not a threshold process, so that the situation in which γ_0 and γ_2 are of the same order of magnitude turns out to be entirely realistic. This in turn means that a small number of depolarizing collisions, with little effect on polarization (if any), will occur during the short interval of time between excitation and emission. An atomic ensemble can be polarized, and this may be reflected in the partial polarization of emission lines, even in the case of dense media in which anisotropic kinetic processes take place. This is a fundamental point because it substantially extends the possible range of existence of polarized states. The phenomenon has been detected experimentally in the plasma of an arc discharge at atmospheric pressure, using the polarization of a number of atomic and ionic lines of inert gases (argon and neon).[13,14] A similar phenomenon has been observed,[101,102] but under somewhat different conditions, by investigating the polarization of laser-induced fluorescence of flames at atmospheric pressure.

Apart from the increase in the contribution of quenching, an increase in pressure produces a change in the kinetics of excited states: direct processes yield to step-wise processes, and radiative kinetics yields to collisional kinetics. At high degrees of ionization, the kinetics of the population of states is determined by electron collisions. The diversity of alignment kinetics is then due to the energy dependence of the anisotropy of the motion of electrons.

To gain a clearer picture of the properties of alignment in collisional plasma, let us consider a simple level scheme consisting of the ground state and a set of excited states. We shall suppose that the energy difference between the ground state and the excited states is large enough to ensure that threshold electrons have appreciable anisotropy. At the same time, the energy difference between the excited states will be assumed to be much smaller than the mean thermal energy of electrons. This situation occurs in inert gases. We shall take the following alignment processes into account in the approximation of diffusive coupling of states[80]:

—excitation from the ground state by direct electron impact

—preferential transfer of excitation between neighboring states

—transfer of excitation by the state (for alignment, this always has to be taken into account when there is a state with $J = 0, 1/2$);

—isotropic collisional relaxation.

In this model, the kinetic equations for alignment are written in the form

$$F_{gi}^{(2)} + \sum_{j=(i\pm1),\ (i\pm2)} B_w(ji)\,\rho^{(2)}(j) - \Gamma_2(i)\,\rho^{(2)}(i) = 0; \quad (3.5)$$

where $\Gamma_2(i)$ includes the probabilities of radiative and radiationless transitions from the state i to all other states, and also the frequency of depolarizing collisions. The quantities $B_w(ji)$ are given by

$$B_w(ji) = (-1)^{J_i+J_j+1}(2J_i+1)\begin{Bmatrix} J_i & J_i & 1 \\ J_j & J_j & 2 \end{Bmatrix} w_{ji}, \quad (3.6)$$

where w_{ji} is the probability of a collisional transition between states j and i. The influx of electrons from the continuum to the state i as a result of recombination should not provide an appreciable contribution to alignment because the recombination process involves mostly thermal electrons whose distribution is nearly isotropic.

The solution of (3.5) for one of the excited states contains a number of terms that can be divided into several groups. The first group contains the term $F_{gi}/\Gamma_2(i)$ that describes direct excitation from the ground state. The second group contains terms of the form $F_{gi}^{(2)}B_w(ji)/\Gamma_2(j)\Gamma_2(i)$, that describe two-quantum transitions. The third group contains terms corresponding to three-quantum transitions.

Analysis shows that the ratio $B_w/\Gamma_2 \sim 0.1$ is smaller by an order of magnitude than the contribution of direct excitation from the ground state. The remaining terms are smaller still:

$$\frac{B_w(il)\,B_w(lj)}{\Gamma_2(i)\,\Gamma_2(l)} \sim 0.01,$$

and so on. Their combined contribution to alignment will be reduced by the further fact that, depending on J_i and J_j, the quantities $B_w(ij)$ can have different signs and partially cancel out. Hence, the longer and the more tortuous the path of the electron between successive states, the less memory remains of the initial order in the angular momenta, i.e., the alignment efficiency is reduced.

This is the fundamental difference between the kinetics of alignment and the population kinetics of excited states. When the role of external processes in the population and depletion of levels is small, the motion of bound electrons in the energy space of the atom may be looked upon as a continuous flow that is constant for all states.[80] However, this is not valid in the case of alignment transfer for the following three reasons: (a) partial depolarization due to the symmetry properties of the transfer process, (b) loss of order in each intermediate state due to depolarizing collisions, and (c) total loss of memory of alignment when a state with $J = 0,1/2$ is reached. The result is that direct processes become sharply more important. This was confirmed experimentally in Ref. 42, which demonstrated the absence of argon-ion alignment in the dc arc discharge at atmospheric pressure.

4. EXPERIMENTAL METHODS FOR INVESTIGATING POLARIZATION EFFECTS

4.1. Polarimetry techniques

As noted above, the polarization of an atomic ensemble manifests itself in the polaization of the radiation emitted by it. The polarization properties of this radiation are investigated in polarimetry. The properties of the radiation emitted by plasma are such that a substantial improvement in polarimetry has become necessary. The polarization composition of this radiation can be very complicated, and little *a priori* information about it is usually available. Since we are normally interested in radiation with a narrow spectral interval, we have to deal with low intensity signals for which photon statistics becomes significant and measurements are performed near the sensitivity threshold. At the same time, even for relatively small fluctuations in radiation intensity, both the temporal and spatial fluctuations in the polarization signal may become significant,[13] which gives rise to a further complication of the measurement problem. It is also important to note that polarization studies, and plasma spectroscopy generally, are based on the solution of ill-posed problems.[103] In the present case, this means that small uncertainties in the measured quantities may correspond to considerable uncertainties in the plasma parameters to be determined. High precision of measurement is therefore a further requirement that has to be satisfied.

We must now formulate the criteria for the measuring equipment used to investigate the polarization of atomic ensembles, based on the above properties of plasma radiation:

— possibility of simultaneous measurement of all the Stokes parameters of fluctuating radiation

— the absence of moving parts and, consequently, rapid response and high precision of measurement

— minimum possible loss of light

— possibility of combination with a high-resolution spectrometer.

Advances in the techniques used to measure the polarization of plasma radiation proceeded for a long time separately from the substantial advances in ellipsometry.[104–106] A large number of different polarimeters[107–114] for plasma studies was developed between the late 1920s and 1970s, but they were all based on the comparison of light intensities with particular orthogonal plane polarizations. The final result was calculated from formulas such as

$$P = \left(\frac{I_\parallel}{I_\perp}\frac{I_\perp^c}{I_\parallel^c} - 1\right)\left(\frac{I_\parallel}{I_\perp}\frac{I_\perp^c}{I_\parallel^c} + 1\right)^{-1}, \quad (4.1)$$

where the superscript c labels calibration measurements. The quantities $I_\parallel$ and $I_\perp$ could be measured simultaneously, so that the experimental arrangement usually employed the splitting of the light flux associated with a particular spectral line into two beams, using polarizing prisms or crystal plates. The radiation passing through the analyzer was recorded simultaneously by two photodetectors (usually photomultipliers), and the signals were fed into a difference circuit. In another method, the intensities with perpendicular polarizations were measured in succession, and were produced by rotating the analyzer.[108,109] It is readily seen that even when instrumental uncertainties are reduced, these methods are suitable only for measurements of high degrees of polarization. The uncertainty in the calculated polariza-

tion P exceeds by a substantial factor the uncertainty in the measured radiation intensity.

The common feature of the above methods, which is a universal source of uncertainty in the measured degree of polarization, is the different transmission of the spectral device for perpendicularly polarized beams of radiation. These uncertainties are usually removed by depolarizing the radiation incident on the entrance slit of the spectrometer. This is done by depolarizing prisms,[112] or suitably oriented quarter-wave plates.[114]

In addition, each scheme has its own particular sources of uncertainty. In the arrangement using beam splitting, uncertainties are due to the nonuniformity of the plasma radiation over the beam cross section as well as differences between optical channels, including differences between the sensitivities of the photodetectors. The last of these can be eliminated by suitable calibration. The arrangement in which the beams of light are recorded simultaneously is preferred in investigations of stationary objects. The specific uncertainties introduced in this method are associated with the nonuniform rotation of the analyzer and beats of its axis. Moreover, when the plasma parameters are subject to strong fluctuations and drift, so that the radiation is similarly affected, this method requires a long averaging time or gives only qualitative results.

A polarization spectrometer for the investigation of low radiation intensities from inhomogeneous plasmas was proposed in Ref. 112 and combines the advantages of the above two methods. The two beams of light with orthogonal polarizations are recorded by channel-switching counting circuits, so that rotating elements are avoided.

The polarimeter described in Ref. 114 employs the simultaneous detection of the radiation fluxes and performs absolute measurements of the degree of polarization for inhomogeneous nonstationary objects with a low level of optical signal. The two orthogonal plane polarizations are separated by a Rochon prism which produces a beam divergence angle of 5.7°.

In addition to the deficiencies of the above methods that we have already mentioned (low precision, low sensitivity, and slow response), they suffer from one further disadvantage. In principle, they are capable of measuring only two Stokes parameters that correspond to plane polarized radiation, and even then they require *a priori* information on the position of the axes of the polarization ellipse. It follows that the quality of the final results always depends on the validity of the adopted assumptions. Moreover, the range of modern techniques used in complete polarimeters, i.e., polarimeters that simultaneously measure all the Stokes parameters, is very restricted. A new Fourier polarimeter for plasma investigations, which satisfies the above criteria was therefore developed.[14] A block diagram of this polarimeter is shown in Fig. 6, and we shall now describe it in detail.

The radiation to be analyzed is collimated and then intercepted by a linear electro-optic modulator (EM) supplied by an alternating voltage from the oscillator OSC. The incident wavefront is then divided into two by the analyzer consisting of the two polarizing prisms P1, P2 mounted so that the optical axes of one them (P1) coincide with the optical axes of the modulator ($\alpha = 0$), whereas the axes of the other are at an angle of 45° to them. Since the polarizing prisms divide the incident radiation into two beams with perpendicular polarizations, the analyzer has four optical outputs. Radiation from these outputs is first wavelength selected and is then intercepted by photodetectors PH1–PH4.

We shall use the Müller matrices to describe the operation of the system. At any of the four analyzer outputs the Stokes vector is a function of the incident-wave Stokes vector $|\eta|$:

$$[\eta'] = [M_A][R(\alpha)][M_\delta][\eta], \tag{4.2}$$

where $[M_A], [M_\delta]$ are the Müller matrices of the analyzer and phase modulator, respectively, and $[R(\alpha)]$ is the rotation matrix. Substituting the corresponding matrices and solving (4.2) for the intensity of light at the analyzer outputs, we obtain

$$2\eta_0' = \eta_0 + \eta_1 \cos 2\alpha + (\eta_2 \cos\delta + \eta_3 \sin\delta) \sin 2\alpha. \tag{4.3}$$

Let us now suppose that the phase angle δ varies periodically with frequency ω. Expanding $\sin\delta$ and $\cos\delta$ into a Fourier series, and neglecting the higher-order harmonics, we obtain the following signals at the four photodetector outputs, respectively:

$$I_1(\alpha = 0°) = \frac{1}{4}(\eta_0 + \eta_1), \tag{4.4}$$

$$I_2(\alpha = 90°) = \frac{1}{4}(\eta_0 - \eta_1),$$

$$I_3(\alpha = 45°) = \frac{1}{4}[\eta_0 + \eta_2(2\tilde{J}_2 \cos 2\omega t + \tilde{J}_0) + 2\eta_3 \tilde{J}_1 \sin\omega t],$$

$$I_4(\alpha = 135°) = \frac{1}{4}[\eta_0 + \eta_2(2\tilde{J}_2 \cos 2\omega t + \tilde{J}_0) - 2\eta_3 \tilde{J}_1 \sin\omega t];$$

where $\tilde{J}_n$ are Bessel functions. It is clear from these equations that only two of the four polarimeter channels need be used to measure the Stokes parameters uniquely. The parameters η_0 and η_1 are determined from the constant component of the photodetector current, η_2 is determined from the component at frequency 2ω, and η_3 from the component at frequency ω. The use of four channels removes the depend-

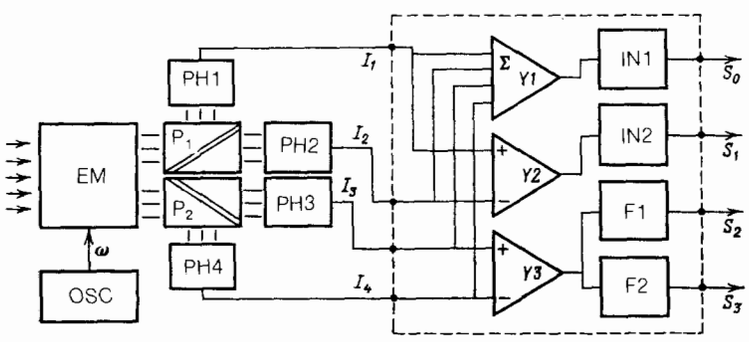

FIG. 6. Fourier electro-optic phase polarimeter.[42,43]

ence of the results on small misalignments, and increases the sensitivity of the instrument. The algorithm used to process the photodetector outputs is based on the simple scheme illustrated in Fig. 6.

Since the optical channels are identical, their transmission characteristics are also identical. The polarimeter can therefore be combined with a spectrometer that has several optical channels and is placed between the polarizing prisms and the photodetectors. The polarization transmission characteristic of the spectrometer must then be taken into account in the relevant equations. The speed of response of the instrument is then restricted by the frequency characteristic of the electrooptic modulator and by the response time of the signal detection system. In principle, a response time of a few tens of nanoseconds can be achieved.

The entire system has to be run by a computer because of the need for higher experimental precision, statistical analysis of several runs, and real-time processing of the data. An apparatus for the investigation of polarization spectra, based on these principles, is described in Ref. 117. It incorporates a somewhat simplified version of the Fourier polarimeter described above, and is capable of measuring the parameters η_0, η_1 and η_2. The electro-optic modulator is a DKDP crystal activated by a high-voltage acoustic oscillator. The analyzer consists of two polarizing prisms with optic axes at 45° to one another. Spectral analysis is performed by a DFC-24 double spectrometer, which analyzes simultaneously the two optical channels. The decoupling between the channels is -50 dB. Two optical-fiber lightguides are mounted on the input slit of the spectrometer and are coupled to cooled photodetectors. Synchronous detection at combination frequencies is used to isolate the useful signal.

The outputs of the synchronous detectors are fed into a CAMAC system working in conjunction with the Elektronika-60 microcomputer. The system records the polarization spectra of individual spectral lines and of segments of the continuum in their neighborhood, and performs a statistical analysis of the data. Examples of the recorded polarization spectra are shown in Fig. 22.

4.2. Magnetooptical method

In the polarization spectrometry of low-pressure gas discharges, the magnetooptical technique is used in addition to the direct measurement of the polarization of spontaneous emission. It is based on the measurement of the polarization of spontaneous emission of an atomic ensemble as a function of a weak magnetic field H applied to a portion of the discharge under investigation. The weak magnetic field modifies the electric and transport properties of the object and destroys the transverse components of the alignment of the quantum states of the particles, so that the spontaneous line emission spectrum is found to exhibit a characteristic dependence of polarization on field strength. This dependence, which we shall also call the alignment signal, is the Hanle effect, well known in atomic physics.[7,22,31,118,119]

The advantages of the magnetooptical method, which is effective for low-current pressure laboratory objects, include the possibility of measuring not only the absolute degree of polarization, but also its dependence on a variable external parameter. Moreover, the form of the signal can be used to investigate (without altering the detection channel) the distribution of local alignment axes in different parts of the plasma, and thus reconstruct the spatial features and the character of the anisotropy of kinetic processes.

We must now analyze the Hanle signal for specific conditions. In the traditional arrangment, the degree of polarization of spontaneous emission in the direction parallel to the external magnetic field is investigated. In the approximation defined by $\rho^{(0)} \gg \rho^{(\varkappa)} (\varkappa > 0)$, the degree of polarization is then given by

$$P(\Omega) = \frac{\sqrt{15}}{2\rho_0^{(0)}} \begin{Bmatrix} 1 & 1 & 2 \\ J_b & J_b & J_a \end{Bmatrix} \begin{Bmatrix} 1 & 1 & 0 \\ J_b & J_b & J_a \end{Bmatrix}^{-1} \times \left(\frac{\Gamma_2^2}{\Gamma_2^2 + 4\Omega^2} \operatorname{Re} \rho_2^{(2)}(0) - \frac{2\Omega\Gamma_2}{\Gamma_2^2 + 4\Omega^2} \operatorname{Im} \rho_2^{(2)}(0) \right), \tag{4.5}$$

where Ω is the Larmor frequency.

Let us now consider in greater detail the simple case of uniaxial alignment $\rho_0^{(2)}(\mathbf{n})$, with principal axis defined by the vector $\mathbf{n}$. In the laboratory frame, the polarization moment $\rho_2^{(2)}(0)$ in zero magnetic field, in which we are interested here, is given by

$$\rho_2^{(2)}(0) = \frac{\sqrt{6}}{4} \rho_0^{(2)}(\mathbf{n}) \sin^2\theta \cdot \exp(2i\varphi),$$

where θ and φ define the direction of the vector $\mathbf{n}$. We then have

$$P(\Omega) = P \frac{1}{1+x^2} - P' \frac{x}{1+x^2}, \tag{4.6}$$

where

$$x = \frac{2\Omega}{\Gamma}, \quad P = P_0 \sin^2\theta \cdot \cos 2\varphi, \quad P' = P_0 \sin^2\theta \cdot \sin 2\varphi,$$

and P_0 is the degree of linear polarization of the radiation emitted by a locally defined ensemble of atoms, observed in the direction perpendicular to the alignment axis[92]:

$$P_0 = \frac{3\sqrt{10}}{8} \frac{\rho_0^{(2)}(\mathbf{n})}{\rho_0^{(0)}} \begin{Bmatrix} 1 & 1 & 2 \\ J_b & J_b & J_a \end{Bmatrix} \begin{Bmatrix} 1 & 1 & 0 \\ J_b & J_b & J_a \end{Bmatrix}^{-1}.$$

The function given by (4.6) is the superposition of Lorentz and dispersion type profiles whose relative contribution to the overall signal is determined by the orientation of the principal alignment axis in the coordinate frame in which the radiation is observed. When $\varphi = 0, \pi/2, \ldots$, we have $P' = 0$ and, according to (4.6), the Hanle signal is purely Lorentzian. When $\varphi = \pi/4, 3\pi/4, \ldots$, we have the pure dispersion type signal. A mixture of the Lorentz and dispersion profiles is observed in all intermediate cases.

Let us now consider the basic arrangement of the polarization spectrometer based on the Hanle effect (Fig. 7). A lens whose optical axis is parallel to the magnetic field is used to focus the image of the source on the entrance slit of the spectrometer. The monochromatic radiation is then split by an interference polarizer into two beams with mutually perpendicular linear polarizations along the x and y axes and the difference signal shown in Fig. 8 is generated.

The signal is recorded by a synchronous detector or a multichannel pulse-height analyzer operating at low counting rates.[31] A modernized version of this system, with synchronous data acquisition and averaging by a computerized measuring complex, was used in Refs. 120 and 189. A periodic stepwise increasing saw-tooth voltage was produced during signal acquisition. The instantaneous value of this ramp was proportional to the magnetic field and, at the same

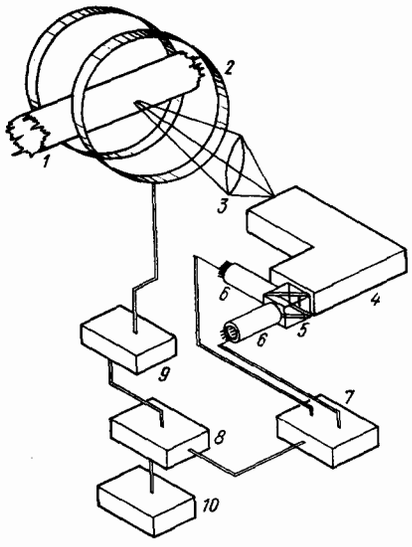

FIG. 7. Functional diagram of a magnetic Hanle spectrometer[189]: 1—source, 2—Helmholtz coils, 3—lens, 4—monochromator, 5—interference polarizer, 6—photodetectors, 7—differential amplifier, 8—measuring and computing complex F-36, 9—current amplifier, 10—stripchart recorder.

time, defined the address of the corresponding channel of the storage unit. With signal acquisition times of 20–30 min, the sensitivity of the system used to measure the degree of linear polarization was of the order of 10^{-4}.

4.3. Inverse problems in polarization spectroscopy

Two problems must be successively solved when the polarization of atomic states is investigated experimentally. First, integrated quantities such as intensities with different polarizations, degrees of polarization, and Stokes parameters must be converted into the corresponding local quantities. The known polarization composition of the radiation emitted by an ensemble of atoms is then used to determine the character of its polarization and to establish its relation to the plasma parameters.

In ordinary spectroscopy, the determination of local quantities from measured integrated quantities involves the

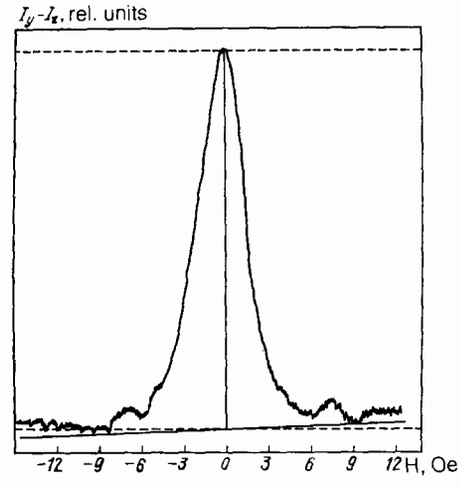

FIG. 8. Typical Hanle signal from the gas-discharge plasma of a capacitive high-frequency discharge in argon, recorded at 763.5 nm (Ref. 189). Field frequency 100 MHz, field amplitude 200 V, gas pressure 8 mtorr.

solution of the Abel type Volterra integral equation of the first kind.[103] There is a number of well known methods that can be used to accomplish this, and we shall therefore not discuss them in detail here.

Formally, polarization measurements do not introduce any fundamental changes into the formulation of the problem. If we measure the degree of polarization, then

$$P(y)=\frac{2}{I}\int_{y}^{R}\varepsilon(r)\,P_2(r)\,r\,(r^2-y^2)^{-1/2}\,dr, \tag{4.7}$$

where $P(r)$ is expressed in terms of the components of the local relative alignment $\rho^{(2)}(r)/\rho^{(0)}(r)$ and we have used the condition $\rho^{(0)}\gg\rho^{(2)}$ which is usually satisfied in plasma physics. It is clear from (4.7) that, to determine $P(r)$, we must know the radial emittance distribution $\varepsilon(r)$. If we use a complete polarimeter, i.e., one that measures simultaneously all the Stokes parameters, we must solve four equations of the form

$$\eta_i(y)=2\int_{y}^{R}\varepsilon(r)\,\tilde{\eta}_i(r)\,r\,(r^2-y^2)^{-1/2}\,dr$$

$$\times\left(\tilde{\eta}_i=\frac{\eta_i}{\eta_0};\ i=0,\ 1,\ 2,\ 3\right), \tag{4.8}$$

one for each of the Stokes parameters.

The determination of local polarization characteristics is seriously complicated by the presence of reabsorption, especially when the absorption coefficients for orthogonally polarized radiation are appreciably different, which occurs, for example, in strong magnetic fields.[121] In general, we have to solve the complicated propagation problem for polarized radiation in a nonisotropic medium.[122]

The measured polarization characteristics of the spontaneous emission of an atomic ensemble are determined not only by the distribution of the radiating atoms within the plasma volume, but also by the variation in the local symmetry properties of the alignment tensor along the line of sight.[92,190] Despite the fact that the problem of reduction to local parameter values is more complicated than in ordinary spectroscopy, modern experimental techniques based on Fourier polarimetry[13] and the magnetooptical technique[189] have successfully solved the problem.

The close connection between the polarization of an atomic ensemble and the kinetic processes that determine the energy and structural properties of a plasma formation can be exploited for diagnostic purposes. For example, when an external source of polarization is present, studies of relaxation processes enable us to determine the temperature or concentration of the perturbing particles.[123] When collisional relaxation is anisotropic, the polarization of the emitted radiation carries information about the even moments of the particle distribution function.[21] It was shown in Section 3 that direct excitation of particles by fast electrons is important, and sometimes decisive, in producing ordered angular momenta of excited states. The alignment tensor, which determines the linear polarization of the emitted radiation, is then related to the electron momentum flux tensor. There is now very considerable interest in the anisotropy of the electron distribution function in different plasma objects, and we shall therefore examine this problem in some detail. With

this in mind, we rewrite (3.2) in the more convenient form

$$\rho_q^{(2)}(i) = N_e \rho_0^{(0)}(g)\,\Gamma_2(i)^{-1} \int_{\mathscr{E}_{ti}}^{\infty} \mathscr{E} Q^{(2)}(\mathscr{E}, \mathscr{E}_{ti})\, f_q^{(2)}(\mathscr{E})\, d\mathscr{E}, \quad (4.9)$$

where i labels the excited states and $\mathscr{E}_{ti}$ is the excitation energy of state i. It follows from (4.9) that the determination of $f_q^{(2)}(\mathscr{E})$ from polarization data requires the solution of an integral equation and, in general, is an ill-posed problem. A review of existing methods for solving inverse problems in plasma diagnostics is given in the monograph of Preobrazhenskiĭ and Pikalov.[103] The inverse problem for the polarization diagnostics of the electron momentum flux tensor was first formulated in Ref. 91. We shall consider a number of formulations of this problem.

When the polarization of several lines has been determined, (4.9) can be looked upon formally as a Volterra equation of the first kind with respect to $f_q^{(2)}(\mathscr{E})$. Its solution provides information on anisotropy in the motion of electrons in the energy range $[\mathscr{E}_1, \mathscr{E}_2]$, where $\mathscr{E}_1$ is the threshold energy and $\mathscr{E}_2$ is the minimum energy at which the integral (4.9) is cut off. An analogous formulation was used to determine the isotropic part of the EDF, $f_0^{(0)}(\mathscr{E})$, from the measured total line intensities due to plasma in coronal equilibrium.[125] When compared with this problem, the case of polarization measurements has two advantages, namely, (a) the cross sections $Q^{(2)}(\mathscr{E})$ and (b) even in a highly collisional plasma, the main source of alignment, in contrast to population, is direct excitation from the ground state, which means that, here again, we can use (4.9). The complicating factor is that the kernel of the integral equation (4.9) does not have a constant sign, which means that the stability of its solutions must be examined separately.

With the same degree of reliability one can determine $f^{(2)}(\mathscr{E})$ from the measured polarization of radiation, using a smaller number of spectral lines. However, this requires independent information about the isotropic part of the EDF. Using (4.9), and recalling that a similar equation can be written for $f_0^{(0)}$ and that

$$\frac{\rho^{(2)}(i)}{\rho_0^{(0)}(i)} = \varphi(P_2),$$

we obtain

$$\begin{aligned}
&\mathscr{E}_{ti} \int_{-\infty}^{\infty} Q^{(2)}(\mathscr{E}_{ti} - \mathscr{E})\, f_q^{(2)}(\mathscr{E})\, d\mathscr{E} \\
&- \int_{-\infty}^{\infty} (\mathscr{E}_{ti} - \mathscr{E})\, Q^{(2)}(\mathscr{E}_{ti} - \mathscr{E})\, f_q^{(2)}(\mathscr{E})\, d\mathscr{E} \\
&= \varphi(P_2) \Big[\mathscr{E}_{ti} \int_{-\infty}^{\infty} Q^{(0)}(\mathscr{E}_{ti} - \mathscr{E})\, f_0^{(0)}(\mathscr{E})\, d\mathscr{E} \\
&\qquad - \int_{-\infty}^{\infty} (\mathscr{E}_{ti} - \mathscr{E})\, Q^{(0)}(\mathscr{E}_{ti} - \mathscr{E})\, f_0^{(0)}(\mathscr{E})\, d\mathscr{E} \Big]
\end{aligned} \quad (4.10)$$

Using the convolution theorem[126] and applying the inverse transformation, we can obtain the required energy dependence of the momentum flux tensor $f_q^{(2)}(\mathscr{E})$. We note that this procedure is also ill-posed and requires the use of the appropriate regularization techniques.

The problem of finding $f_q^{(2)}(\mathscr{E})$ can be substantially simplified and converted into a well-posed problem when *a priori* information is available about the form of this function. Measurements of the polarization of several lines in the emission spectrum can then be used to determine a similar number of parameters characterizing $f_q^{(2)}(\mathscr{E})$, or to ensure higher precision in the determination of one parameter.

Whatever the particular formulation of the inverse problem, reliable values of the alignment excitation cross sections must be available if the momentum flux tensor is to be determined. Unfortunately, although the literature devoted to the excitation cross sections of different atomic states is quite extensive, there are no direct measurements or theoretical calculations of this quantity. Nevertheless, $Q^{(2)}(\mathscr{E})$ can be determined from experimental data taken from other fields of research, namely, electron-photon coincidences,[127] or the excitation of atoms by monoenergetic electron beams,[73] in which the degree of polarization of fluorescence is determined as a function of the energy of the incident electrons. However, both types of experiment cover only a limited number of states of different elements.

In this connection in Ref. 128 a relatively simple approximate method has been developed for calculating the cross section $Q^{(2)}(\mathscr{E})$. It makes use of the extensive theoretical and experimental data[72,129,130] on the inelastic differential electron scattering cross section $Q(\chi, \mathscr{E})$. The calculation is based on isolating from $Q(\chi, \mathscr{E})$ the quadrupole part in the coordinate frame in which the z axis lies along the momentum vector $\mathbf{K}_e$ (see Fig. 2), and then transforming the resulting tensor to the laboratory frame. Conservation of momentum

$$K_e^2 = k_e^2 + k_e'^2 - 2k_e' k_e \cos\chi$$

and conservation of energy

$$\frac{k_e'}{k_e} = \left(\frac{\mathscr{E} - \mathscr{E}_i}{\mathscr{E}}\right)^{1/2} = (1 - \delta_{\mathscr{E}})^{1/2} \quad \left(\delta_{\mathscr{E}} = \frac{\mathscr{E}_1}{\mathscr{E}}\right)$$

in the electron-atom collision then lead to the following computational formula:

$$\begin{aligned}
Q^{(2)}(\mathscr{E}) = (-1)^J C^{20}_{J0J0} \int_0^{\pi} (3\cos^2\chi - 1) \\
\times \Big[2 - \frac{3\sin^2\chi}{2 - \delta_{\mathscr{E}} - 2(1-\delta_{\mathscr{E}})^{1/2}\cos\chi} \Big] \\
\times Q(\mathscr{E}\chi) \sin\chi\, d\chi.
\end{aligned} \quad (4.11)$$

As an example, Fig. 9 shows the cross section $Q^{(2)}(\mathscr{E})$ calculated from the differential cross sections for two states of the argon atom. The energy dependence of the differential cross sections in these states was taken from Ref. 131.

The extensive available data on intermediate-energy electrons can be used to calculate $Q^{(2)}(\mathscr{E})$. At high electron energies, the Born approximation gives good results. An analytic expression can then be found for $Q^{(2)}(\mathscr{E})$ by using (2.7) for the cross section $Q^{(2)}$ and the angle ψ (Fig. 2). It is shown in Ref. 71 that, for optically allowed transitions and high electron energies,

$$\langle \cos^2\psi \rangle = \ln^{-1} \frac{\mathscr{E}}{B_1},$$

whereas for forbidden transitions[72]

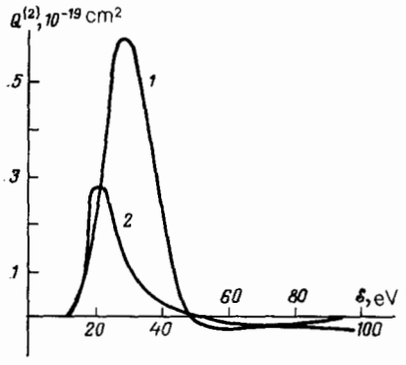

FIG. 9. Cross section for alignment by electron impact in the case of the $2p_4$ (1) and $2p_0$ (2) states of argon[91] as a function of energy.

$$\langle \cos^2 \psi \rangle = \frac{B_2}{\mathscr{E}},$$

where B_1 and B_2 are certain constants. The electron energy $\mathscr{E}_0$ at which $Q^{(2)}(\mathscr{E})$ changes sign is a more convenient parameter than B_1 and B_2. It follows from (2.7) that this energy corresponds to the condition

$$\langle \cos^2 \psi \rangle = \frac{1}{3}.$$

Expressing B_1 and B_2 in terms of $\mathscr{E}_0$, we obtain

$$Q^{(2)}(\mathscr{E}) = \frac{C^{20}_{J0J0}}{C^{00}_{J0J0}} \left[1 - \frac{1}{1+(1/3)\ln(\mathscr{E}/\mathscr{E}_0)}\right] Q^{(0)}(\mathscr{E}) \quad (4.12)$$

for allowed transitions and

$$Q^{(2)}(\mathscr{E}) = \frac{C^{20}_{J0J0}}{C^{00}_{J0J0}} \left(1 - \frac{\mathscr{E}_0}{\mathscr{E}}\right) Q^{(0)}(\mathscr{E}) \quad (4.13)$$

for forbidden transitions.

Therefore, by calculating $Q^{(0)}(\mathscr{E})$ from the Born formula,[129] and by determining $\mathscr{E}_0$ from a preliminary calculation based on (4.11), we can extend the function $Q^{(2)}(\mathscr{E})$ to energies $\mathscr{E} > \mathscr{E}_0$.

5. POLARIZATION SPECTROMETRY OF IONIZED GASES

5.1 Positive column of the glow discharge

We now turn to the polarization of atomic ensembles in particular objects, and begin with one of the simplest laboratory sources of low-temperature plasma, namely, the low-pressure dc gas discharge. This object has been extensively investigated both experimentally and theoretically,[132,133] and is therefore of interest from a methodological point of view.

There is an extensive series of publications[33,34,124,134–143,193] devoted to polarization studies of the dc discharge. The experiments were carried out in inert gases, using a magnetic polarization spectrometer. The alignment of 2p states corresponding to different degrees of excitation was studied by analyzing the Hanle signal as a function of the discharge conditions. For neon pressures 0.3–10 torr,[34,134,135] argon pressures 0.2–2 torr,[136–139] krypton pressures 0.05–0.3 torr,[140,141] and xenon pressures 0.01–0.05 torr,[142,143] the alignment signal could be satisfactorily described by a Lorentz curve, whose parameters were determined by the relaxation time of the upper state involved in the atomic transition. At lower pressures, the signal was found to have a narrow component of opposite sign, whose

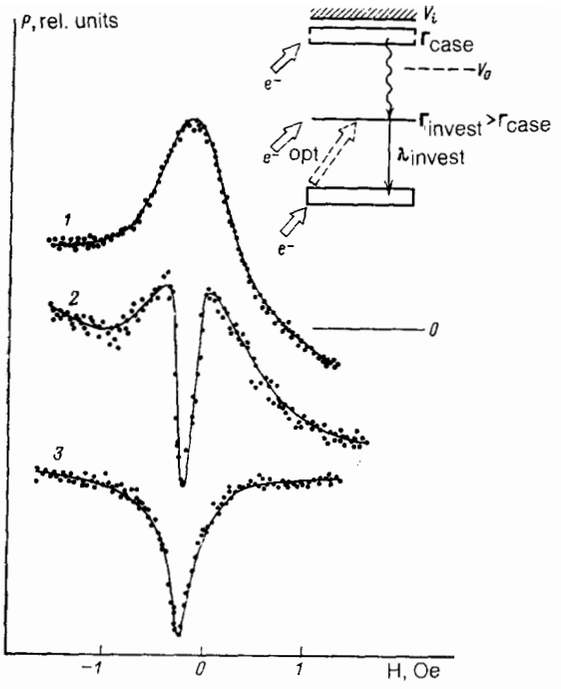

FIG. 10. Hanle signals due to the $2p_2$ level of krypton ($\lambda = 587.1$ nm) in the positive column of a dc discharge as function of pressure.[141] P = 100 (1), 30 (2), and 20 (3) mtorr; discharge current 30 mA.

amplitude increased with decreasing pressure. At the same time, the relative contribution of the broad component decreased, and vanished altogether at the lowest pressures. Figure 10 shows typical alignment signals due to transitions from the $2p_2$ state of krypton at different pressures. This behavior suggested that the two components of the complex signal had a different physical origin.[197] The broad component was found to be related to the alignment of the 2p state as a result of the reabsorption of the resonant radiation in 1s–2p transitions.[33,34] As the pressure was reduced, the reduction in the population of atoms in the intermediate 1s states, in which the resonance radiation was absorbed, was accompanied by a reduction in the efficiency of this mechanism.[138,144] The signal of opposite sign was due to the cascade transfer of alignment, which was confirmed by the observed alignment of highly-excited states that were optically related to those considered here.[141,196] This selective alignment of states with energies exceeding a particular value has been observed at pressures of 0.07–0.7 torr[194] in neon, at 0.015–0.3 torr in argon,[195] and at 0.004–0.08 torr in xenon and krypton.[145] Subsequent analysis showed that, at low pressures, the alignment of atoms in the positive column of the discharge should be related to the anisotropy in the motion of exciting electrons and not to resonance photoexcitation. At the same time, the absence of alignment of the deep p-states indicated that, at lower energies, the motion of the electrons was nearly isotropic. Detailed examination of alignment and emission signals from peripheral regions, and observations on the discharge axis, yielded the distribution of alignment by electron impact within the discharge (Fig. 11).

The qualitative picture of electron kinetics in the positive columns at low pressure, deduced from polarization measurements, is as follows. A large potential discontinuity V_0 occurs across the plamsa-wall boundary. Slow electrons

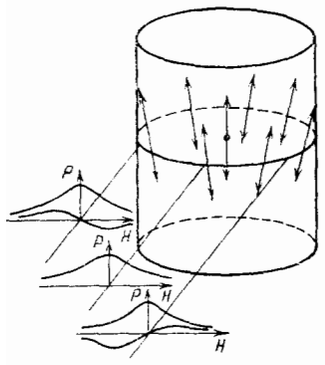

FIG. 11. Spatial distribution of alignment by electron impact in the positive column of a dc discharge, and variation of the Hanle signal.[120]

with energies lower than the wall discontinuity are reflected elastically from it, and their motion can be regarded as weakly anisotropic. For particles with energies exceeding V_0, and moving at right angles to the wall, there is a nonzero probability that they will escape from the plasma and will be lost to the pipe wall in a time $\tau \sim R/v_f$. The resulting deficit of fast passing electrons, with velocities perpendicular to the wall defines the loss cone in the velocity distribution of fast electrons, which in turn leads to the energy selectivity of alignment.[188] Control experiments with an electron beam have confirmed that the high-energy states are excited by electrons moving preferentially along the axis of the discharge. The deviation of the alignment axes from the axial direction, and the effect of the discharge current on the deviation angle, are a consequence of the fact that the radial electric field in the column leads to the rotation of the loss cone through a small angle.[146] Since the characteristics of the loss cone in a given cross section are determined by the local value of the potential, the potential distribution in the plasma can be estimated by investigating the distribution of the polarization of excited atoms in the radial direction.[191]

5.2. High-frequency capacitive discharge

Despite the long history of research into physical processes occurring in the high-frequency low-pressure discharge, these phenomena are still the subject of constant discussion in the literature.[147] In an earlier series of theoretical papers, the properties of the plasma in the high-frequency discharge were analyzed in terms of the Boltzmann transport equation, using a sufficiently general approximation that provided no hint of unexpected features. The electrons were thought to oscillate relative to the stationary atoms and ions with the oscillation frequency being equal to the field frequency. The oscillating electrons received energy from the field, which was converted into thermal energy by collisions. The result was an almost Maxwellian distribution function, with a weak anisotropy along the field. However, subsequent experimental examination of the discharge near the electrodes revealed the presence of strong constant electric fields whose magnitude could not be explained by ambipolar particle diffusion.[148] Measurements of the potential distribution in the plasma within the discharge gap showed that, when the field frequency was much lower than the electron plasma frequency, the field was localized near the electrodes. The interaction between the high-frequency voltage and the wall discontinuity in the potential has a number of important consequences.[149] Because the current-voltage characteristic of the layer near the electrodes is nonlinear, the high-frequency voltage becomes rectified, and this increases the constant potential difference between the medium and the electrode (or the dielectric wall in the case of a discharge with external electrodes). Electrons entering the boundary region acquire further energy and their motion becomes anisotropic in the direction perpendicular to the electrodes. Thus, a group of fast electrons with velocity anisotropy was recorded in Refs. 150 and 151, and was interpreted as a quasibeam propagating towards the center of the discharge. It is precisely these electrons that are found in the tail of the distribution function and provide the maximum contribution to direct ionization and excitation of neutral particles. At the same time, they can lead to the alignment of the states of these particles. The polarization of the spectral lines emitted by them must then increase in the direction between the center of the discharge and the electrodes.

Polarization studies of the E-type high-frequency discharge in inert gases were performed in Refs. 12, 36, and 115 by the magnetooptical method. The discharge was maintained in spherical vessels 3.5 and 4 cm in diameter. The frequency of the alternating field was 100 MHz. The gas pressure in the vessels was varied in the range 0.02–3 torr.

The physical nature of the alignment of excited atoms was investigated in preliminary experiments, using the difference between the symmetry properties of resonance photoexcitation and the distribution function of exciting electrons. At pressures of 0.1–2 torr, the spatial distributions of the degree and direction of polarization, and also of the radiation intensity, were close to those expected for the optical alignment mechanism, i.e., they were spherically symmetric. The measured absorption coefficients were also found to support the optical mechanism.[198] When the pressure was reduced to 0.1 torr or less, the intensity distribution obtained for all the spectral lines was found to tend to the uniform distribution independently of the excitation energy, and there was an increase in the degree of polarization of the radiation emitted by the central part of the discharge. This suggested a greater rôle of direct electron excitation in the production of alignment.

Polarization measurements on the 794.8 and 811.5 nm argon lines in the central part of the discharge were reported in Ref. 91 in the case of alignment by electron impact. The data were then used to determine the amplitude of the alternating electric field. Assuming that the zero-order moment of the distribution function was Maxwellian with a temperature of about 5 eV (Ref. 152), and that the anisotropic EDF was determined by the high-frequency electric field, it was found that the electron momentum flux tensor could be written in the form[90]

$$f_0^{(2)}(\mathscr{E}) = A\mathscr{E} f_0^{(0)}(\mathscr{E}),$$

where

$$A = \frac{2(eE)^2}{m_e T_e^2 (\omega_0^2 + \nu_{ea}^2)}.$$

Substitution of this expression into the Boltzmann equation then yielded the magnitude E of the electric field, which was found to agree with probe measurements performed under similar conditions.[152]

An increase in the degree of polarization near the electrodes had already been found in spherical low-pressure dis-

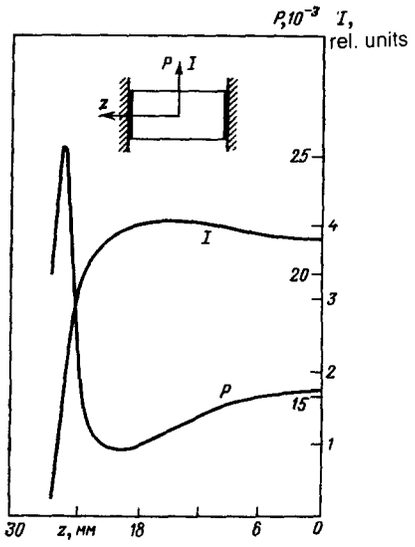

FIG. 12. Polarization anomalies near the electrodes in the radiation from a cylindrical capacitive high-frequency discharge in argon at 100 MHz ($\lambda = 603.2$ nm, gas pressure 5 mtorr).[153]

charges. The region near the electrodes was investigated in greater detail in a cylindrical discharge in which the distribution of radiation had a well-resolved structure reflecting the nonuniformity of the object. A dark space was observed near the electrodes. Its thickness amounted to a few millimeters and was found to increase rapidly as the pressure was reduced. At pressures in excess of 15 mtorr, a maximum was observed on the intensity distribution of spectral lines along the discharge axis near the boundary of the dark space. This maximum was found to broaden and shift towards the center as the pressure was reduced. At pressures below 15 mtorr, the axial density distribution became monotonic. The polarization distribution was also found to have a sharp peak that lay closer to the electrode than the intensity maximum (Fig. 12). The degree of polarization rose with decreasing pressure, and the polarization maximum shifted towards the center. An increase in the degree of polarization was observed throughout the discharge as the high-frequency voltage was increased, but the position of the maximum remained unaltered.

The interpretation of these observations, which indicate that processes occurring near the electrodes play a dominant part in forming the anisotropy in the motion of electrons, is given in Ref. 153 in terms of the following model. The high-frequency field is localized in the layer near the electrodes and amounts to a few hundred V/cm. The layer consists of an oscillating space-charge that is practically free of electrons, and the concentration of ions is close to the mean over the discharge.[154–155] The boundary layer oscillates with the frequency of the external field and amplitude equal to one-half of the layer thickness. The fall in electric potential near the boundary of the positive space charge is so rapid that most of the plasma electrons are reflected elastically from the layer boundary and do not enter it. The result is a quasibeam propagating away from the electrodes and toward the center of the discharge.[156,199] The electron distribution function in the electrode layer that corresponds to this model was used in Ref. 192 together with polarization measurement to estimate the power transferred to the discharge, and to construct the energy balance for the object.

5.3. The region of interaction between a moving plasma and a gas

Polarization spectroscopy was used in Refs. 113, 114, 157, and 158 to investigate the non-steady-state interaction between a beam of hydrogen plasma and a cloud of neutral helium in a magnetic field. The interest in such objects lies outside the scope of purely laboratory problems, and is due to their similarity to astrophysical systems. The evolution of the ionization of a neutral gas, the particle kinetics, and the electron heating mechanisms have been examined by Alfven[159] as processes governing the formation of the solar system.

In the above experiments, a cloud of plasma was formed in an electrodeless plasma gun and traveled along a drift tube in a constant magnetic field. The magnetic field strength did not exceed 5 kG, and its direction at the end of the drift tube was perpendicular to the beam axis. The particle density in the beam was 10^{11}–10^{12} cm^{-3} and the beam velocity on entry into the gas was 500 km/s. The dimensions of the helium cloud were $5\times5\times5$ cm^3 and its pressure was 3 mtorr. The frequency of electron–atom collisions in these experiments was of the order of the reciprocal of the time of interaction between the plasma and the gas, i.e., 1.3×10^4–50×10^4 s^{-1}. This meant that the only significant collisions were those between free electrons and helium atoms.

These experiments resulted in the discovery that a number of the HeI lines were polarized (501.6, 492.2, 471.3, and 438.2 nm). The degree of polarization of the radiation emitted as a result of ^{1}D-^{1}P transitions was about 7%. Figure 13 shows the primary data for the 492.2-nm line. The direction of preferential polarization corresponded to the alignment of ^{1}D states by a beam of fast electrons moving along the magnetic field. This excitation geometry ensured that there was no depolarization by the magnetic field, and there was no distortion of information on the anisotropy of the moving electrons.

Comparison of these experimental results with independent polarization data on the spontaneous emission of helium excited by a beam of monoenergetic electrons,[160,161] and also parallel spectroscopic observations, showed that the energy of the electron beam produced in the interaction region was close to 100 eV, whereas the energy of plasma electrons was of the order of 5 eV. The difference between the measured polarization and the maximum possible at 100

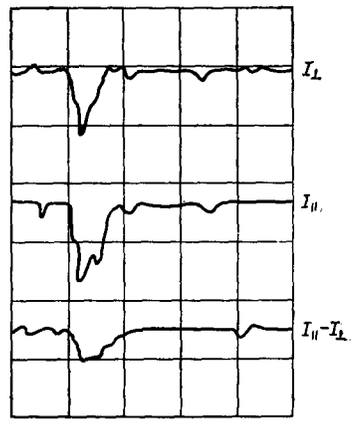

FIG. 13. Pulsed polarization signals recorded for the 492.2-nm helium line.[113,114]

eV was an indication of the presence of randomly moving intermediate-energy electrons that could also participate in the excitation of states.

These experimental results lead to a model of the plasma-gas interaction. According to this model, helium ions are produced by direct ionization when the hydrogen beam is injected into the gas. These ions excite plasma instabilities with the accompanying strong electric field. Ions produced as a result of secondary ionization are accelerated by the electric field and, in turn, maintain this field. It is precisely this phenomenon that is thought to be responsible for the rapid deceleration of the plasma beam from 500 km/s at entry into the gas down to 40 km/s in the interaction region. The gas remains neutral outside this region, and excess charge accumulates on its boundary. This charge is responsible for the potential discontinuity at the boundary. The electrons are trapped in the resulting potential well, and reflections from the walls of the well produce the heating of electrons and the formation of the observed electron beams.

5.4. Gas-filled diode

Several studies of polarized radiation produced in the narrow gap of a cesium diode in a longitudinal magnetic field were published in the late 1970s. These experiments were performed under different conditions, ranging from the Knudsen discharge[40] ($p \sim 5\times10^{-3}$ Torr, $i \sim 0.1$–0.3 A/cm^2) to the quasi-vacuum state[41] ($p \sim 5\times10^{-4}$ Torr, $i \sim 3$–4 A/cm^2). In all cases, the polarization of the emitted radiation was explained in terms of the nonuniform population of magnetic sublevels (polarization of states) due to excitation by fast electrons with an anisotropic distribution function. Since the electrons accelerated in the gap between the electrodes traveled along the magnetic lines of force, the alignment axis and the magnetic field vector were parallel, and there was no depolarization. The magnetic field strength H was chosen according to the condition

$$\Omega > \Delta\omega_{im}$$

($\Delta\omega_{im}$ is the collisional broadening of the spectral line under investigation) with the view to reducing collisional depolarization when the degeneracy of the magnetic sublevels was lifted. The field amounted to about 1 kG.

In the Knudsen discharge, the distribution of the polarization of states was as follows. There were two groups of electrons in the diode gap, namely, quasi-Maxwellian electrons and beam electrons. The first group consisted of electrons trapped in the potential well in the gap[162,163] and Maxwellized by reflections from the walls of the well. The anisotropy was due to the loss cone in the velocity space for electrons with energies in excess of the anode potential discontinuity. The second group of electrons was due to beam instability.[164] The polarization of the plasma radiation emitted by this plasma should be determined by the influence of each of these groups of electrons on the relative population of magnetic sublevels of excited states. The preferred channel for the production of alignment was estimated from the balance of populations of the individual sublevels, taking into account direct, stepwise, and cascade population, and also the effect of collisions of the second kind. The most significant were transitions from the ground ($6S_{1/2}$) and resonance ($6P_{3/2,1/2}$) states of CsI. Since the excitation energy was greater than the anode potential discontinuity, the states were populated by electrons from the first group.

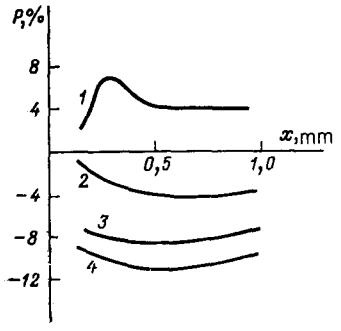

FIG. 14. Spatial distribution of polarization emitted by cesium plasma in the Knudsen discharge at 672.3 nm in a narrow gap in a magnetic field of 310 G (Ref. 40). $U_a = 9$ V, cesium vapor pressure 0.04 torr, current $i = 12$ (1), 100 (2), 120 (3), and 380 (4) mA.

An experimental study was made of the polarization of radiation emitted as a result of $nD_{5/2,3/2} \rightarrow 6P_{3/2,1/2}$ transitions. The measured spatial distribution of polarization is shown in Fig. 14 for different discharge currents. Curve 1 corresponds to the initial discharge for which the width of the cathode space is small, and there is no potential well in the gap. The atoms are excited by electrons whose energies are determined by the potential in the particular cross section of the gap, and the form of $P(x)$ reflects both the distribution of potential and the function $P(\mathscr{E})$. A potential well appears in the gap as the discharge current increases, and this leads to the formation of a quasi-Maxwellian group of electrons. Model EDFs were then used to calculate $P(x)$. It was found that the degree of polarization changed sign as the current increased, and this was confirmed by measurements. However, the estimated values of P were lower than the measured values. This discrepancy was explained (1) by the influence of the magnetic field, i.e., the Paschen-Back effect in the hyperfine structure, (2) trapping in the gap of exciting electrons traveling at large angles to the discharge axis, whose effect on the second moment of the EDF can be considerable, and (3) different reabsorption of radiation with polarization respectively parallel and perpendicular to the magnetic field. A further item that can be added to this list is the possible additional polarization of states due to the difference between the cross sections for the excitation of magnetic sublevels, which arises when their degeneracy is lifted,[165,166] but was not analyzed by the authors of Refs. 165 and 166.

As lower pressures are approached, the form of the EDF begins to be determined by the boundary conditions on the surface of the electrodes. Figure 15 shows the experimental distributions of P along the axis of the diode for different anode voltages, where $\mathscr{E}(x) = eU_a x/d$ (U_a is the anode voltage, d is the separation between the electrodes and x is the position coordinate along the discharge axis). These distributions should correspond to the function $P(\mathscr{E}^*)$, redefined with allowance for the energy resolution $\Delta\mathscr{E}$. However, comparison of the distributions obtained for different U_a shows that a reduction in the anode voltage leads to a reduction in the degree of polarization, and this is more appreciable as the cross section corresponding to the energy $\mathscr{E}$ approaches the anode surface. This was explained by the influence of secondary electrons arriving from the anode

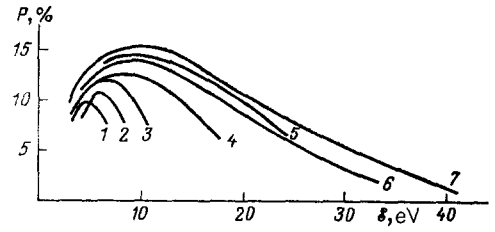

FIG. 15. Polarization of one of the cesium lines as a function of position along the axis of a vacuum diode for different anode voltages (V): 6 (1), 9.2 (2), 12 (3), 20 (4), 28 (5), 40 (6), and 50 (7) (Ref. 41).

surface, whose distribution function is made isotropic by reflections.

5.5. Beam-plasma discharge

The beam-plasma discharge is of interest not only as a laboratory object, but also for studies of phenomena such as the injection of high-intensity electron beams into a gas or plasma, and the entry of charged particles into the upper atmosphere, which gives rise to polar auroras.

Polarization studies of the beam-plasma discharge have been carried out[37] in helium under the following conditions: $p = 10^{-3} - 10^{-2}$ torr, $i = 25$–100 mA. The measurements were made near the wavelengths of 387.0, 401.0, 501.0, and 667.0 nm at half-widths of 6–10 nm. The polarization of the radiation was detected only in the second spectral interval, in which it reached 40% (Fig. 16). This degree of polarization could only have been due to the transition $4^1P_1 \rightarrow 2S_0 (\lambda = 396.5$ nm with an excitation potential of 23.6 eV. Analysis of HeI kinetics in this object[167] has shown that the nonequilibrium population of the magnetic sublevels of the 4^1P_1 state was due to direct electron impact.

The anisotropic motion of fast electrons in the beam-plasma discharge is the result of their interaction with intense plasma oscillations[168,169] which, in the stationary regime, are localized in a bounded volume (HF region) much smaller than the dimensions of the plasma. Under these conditions, charged particles can be trapped near the minimum of the high-frequency potential because of the transfer of the energy of directed motion to the oscillations.[170,171] Because the beam diameter is limited, a transverse component of the high-frequency field is found to appear, and its distribution in space has a minimum on the axis of the system. Estimates show that the longitudinal and transverse components are comparable in magnitude. It follows that the high-frequency field of the beam-plasma discharge gives rise to at least one

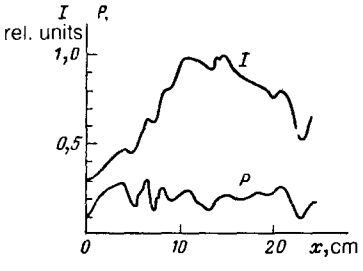

FIG. 16. Axial distribution of total intensity and polarization of spectral lines emitted by the plasma in a beam-plasma discharge in the case of continuous beam injection.[37]

two-dimensional potential well for the plasma electrons. If, on the other hand, the electron energy exceeds the radial potential barrier, the only trapped electrons are those for which the velocity vector lies within the trapping cone, the angle of which depends on velocity. Consequently, electrons both in the high-frequency region and those leaving it acquire anisotropic motion. Since the length characterizing the loss of momentum by fast electrons in Coulomb and elastic interactions is much greater than the dimensions of the beam-plasma discharge, a change in the direction of motion of the electrons is possible only by reflection from the potential barrier on the plasma boundary. It follows that each particular plasma volume should contain two groups of electrons with significantly different distribution functions. One of them consists of electrons trapped in the potential well, and has a nearly isotropic distribution, whereas the other consists of fast electrons that receive energy from the high-frequency field and have an anisotropic angular distribution which depends on the position of the selected volume relative to the high-frequency region and the plasma boundaries. Evidently, it is these electrons that ensure ionization and excitation of atoms in the region in which there are no powerful high-frequency fields that produce the alignment of the 4^1P_1 state and the polarization of 396.5-nm radiation.

5.6. Plasma produced by an electron beam

Technological applications of relativistic electron beams (REB) and of the plasma produced by them involve the injection of such beams into a gas.[172] An important characteristic of the beam-plasma system is the electron velocity distribution function whose anisotropic properties determine entirely the conditions of interaction.

Until quite recently, experimental studies of the electron distribution function in such systems were limited by the possibilities of probe methods. The first, and so far the only, experiments on the investigation of the anisotropy of the electron distribution function in the plasma produced by a relativistic electron beam are those reported in Ref. 43, where the methods of polarization spectroscopy were employed. The experiments were performed using a relativistic electron beam with the following parameters[173]: electron energy 350 keV, current 15 A, pulse length 40 μs. The beam was injected into a drift chamber 30 cm in diameter and 1 m long, filled with argon to a pressure of 25 Pa through a 1.4-cm diameter valve. The electron density on the beam axis was $\sim 2 \times 10^9$ cm^{-3} and the plasma electron density was $\sim 10^{11}$–10^{13} cm^{-3}. Pulses of radiation in the 488.0-nm ArII line were examined in orthogonal polarizations (Fig. 17). Figure 18 shows the radial distribution of polarization in this line. Positive values correspond to polarization pointing along the radius of the relativistic electron beam. The figure indicates the uncertainties that characterize the reproducibility of these measurements and correspond to a 90% confidence interval.

The following simple model was put forward to explain these results. Atoms are ionized by impact when the electron beam is injected into the tenuous gas. Secondary electrons in the first-generation cascade are emitted preferentially across the direction of the beam (Fig. 19), leave the beam, and are accelerated in the radial direction by the electric field of the space charge. At the same time, the ions are trapped in the potential well.[174] This process continues until a dynamic

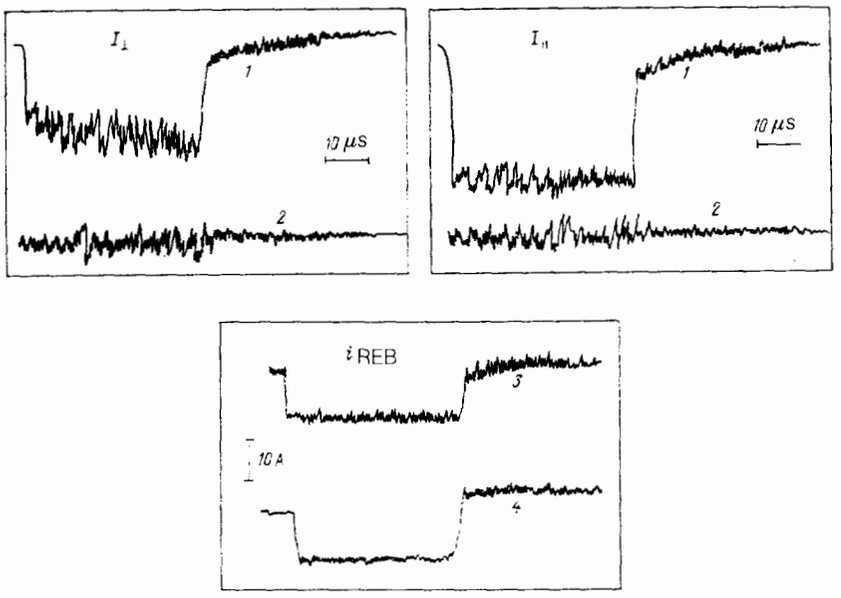

FIG. 17. Oscillograms of pulses of radiation emitted by ArII ions at 488.0 nm in the region of injection of a relativistic electron beam ($I_\parallel$, $I_\perp$) and the corresponding current pulses I_{REB} (Ref. 43). 1—line intensity pulse, 2—plasma noise, 3—Faraday cylinder, 4—Rogowski belt.

equilibrium is established between the rate of escape of ions and electrons from the beam localization region and the rate at which they are produced. In the steady state, the positive ion space charge compensates the negative beam charge, so that the system as a whole becomes effectively neutral, which reduces the effect of the radial electric field. When the beam pulses are long enough, complete neutralization can occur at the above gas densities, but only for the beam as a whole: as a rule, there is no *local* neutralization.[175] An excess negative charge appears on the beam axis during this process. Consequently, electrons near the beam axis will, as before, experience a radial electrostatic force, but on the boundary they will experience mostly the thermal and magnetic pressures.

Secondary electrons are more effective in ionizing the gas because their energy is lower than the energy of the beam electrons, and the corresponding ionization cross section is higher. The mean free path is 0.5 cm for $\mathscr{E} \approx 1$ keV and 0.2 cm for $\mathscr{E} \approx 100$ eV, so that secondary electrons experience between two and five collisions as they move in the radial direction in the channel. Electrons in the first-generation cascade, which undergo strong collisions with atoms, play a dominant part in ionization with excitation. These electrons are scattered through small angles, so that the angular part of their distribution function changes only slightly, and their energy is reduced.

As far as the magnetic field due to the beam current itself is concerned, we find that, as the necessary plasma density is being established during the injection process, the electric and magnetic fields associated with the beam front induce a reverse current that produces a current, and, consequently, a magnetic neutralization. In the course of time (usually after a few tens of nanoseconds), this neutralization becomes weaker but, as before, the magnetic field has little effect on the angular part of the electron distribution function because the Larmor radius is much greater under these conditions than the transverse size of the interaction region for all the electron groups. It follows that the secondary-electron distribution function integrated over the current

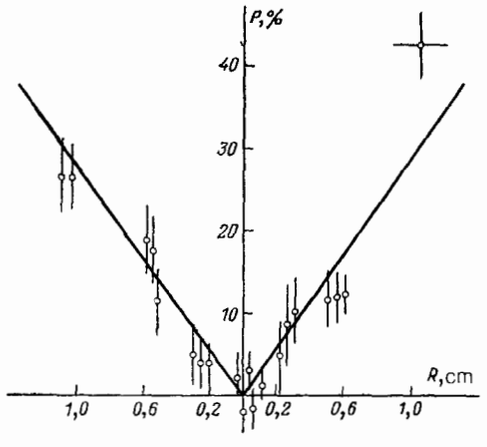

FIG. 18. Radial distribution of the polarization of radiation emitted by REB plasma at 488.0 nm (ArII).[43]

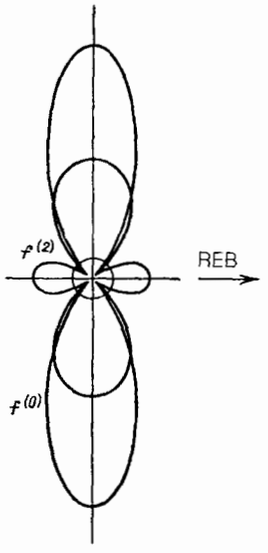

FIG. 19. Typical angular distributions of secondary electrons.[43]

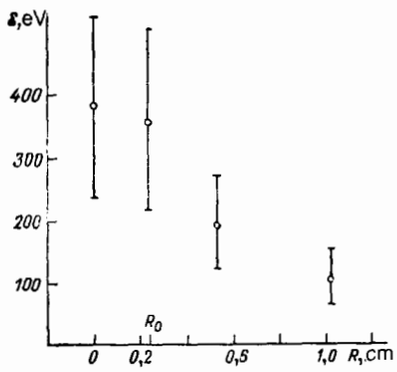

FIG. 20. Reconstructed radial energy distribution of secondary electrons in plasma produced by a relativistic electron beam.[43]

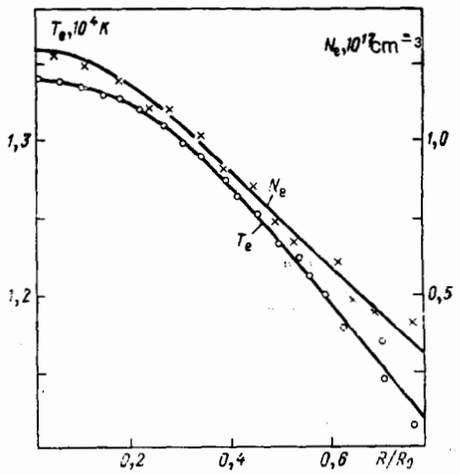

FIG. 21. Radial distributions of plasma parameters in an arc discharge at atmospheric pressure.[13,14]

pulse is anisotropic, with its axis lying along the beam radius.

To determine this anisotropy from polarization measurements, we must establish, as before, the excitation channels for the 4p states of the ArII ion. Estimates show that of the three possible mechanisms, i.e., direct electron impact in the ground state of an atom, or ion, and cascade transitions from higher-lying levels, direct electron impact with simultaneous ionization and excitation of the argon atom is the most likely. Clearly, the alignment of ionic states will also occur in this process. Since there are no direct measurements, the alignment cross sections have been estimated[43] using a model polarization function $P(\mathscr{E})$ for a collimated beam of monoenergetic electrons (Section 2.2). The experimental function $P(R)$ was then converted into the radial distribution $\mathscr{E}(R)$ of the average energy of secondary electrons for these conditions (Fig. 20). It is clear from the figure that the average energy of radially moving secondary electrons decreases with increasing distance R: it amounts to 400 ± 100 eV in the region of localization of the relativistic electron beam, and falls to 110 ± 30 eV at a distance of 1 cm. This method is sensitive between the excitation threshold ($\sim$35 eV) and the $\sim$1 keV limit. Thereafter, the degree of polarization is insensitive to further increase in the electron energy.

5.7. Arc discharge at atmospheric pressure

Polarization of atomic ensembles is usually investigated in low-pressure plasmas. It had been considered that collisional processes destroyed alignment as the pressure was increased. However, observations of atmospheric pressure plasmas[13,14,42] have forced a review of established ideas and have shown that the polarization of states in collisional media not only exists, but can be quite considerable.

Studies of the polarization of states in dense media require a medium that has been well investigated in all other respects. The dc arc discharge is the most convenient from this point of view because all its basic parameters have been determined by existing methods,[176–179] and are known accurately. The radial distributions of electron temperature and concentration are shown in Fig. 21 for an arc current of 42 A. The experiments were performed in argon and in a mixture of neon and 1% argon. Figure 22 shows typical polarization spectra for the emission lines of argon atoms and ions. The radial distributions of the Stokes parameters were obtained for different discharge currents in 24 spectral lines of ArI, ArII, and NeI. Figure 23 shows the degree of polarization for three emission lines from the axial part of the plasma as a function of current. Analysis of an extensive volume of experimental data has shown that

—the direction of anisotropy at the center of the arc is the same as that of the discharge axis

—the polarization of radiation emitted as a result of transitions from levels with angular momenta 0 and 1/2 is much lower than that due to other levels, and is comparable with the measurement uncertainties

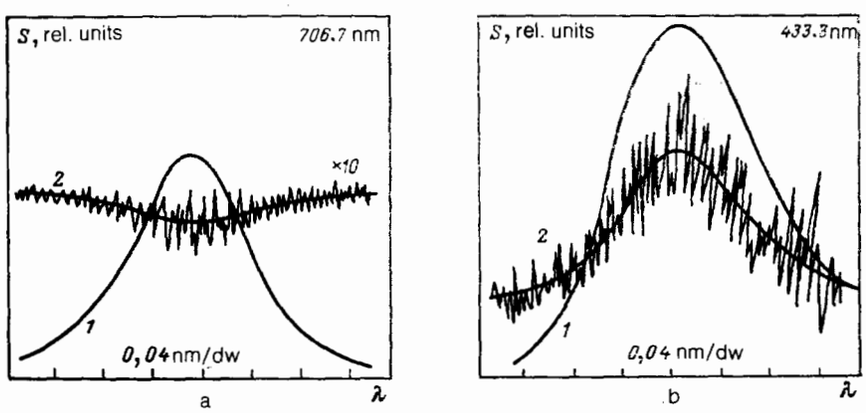

FIG. 22. Typical polarizations recorded in the line emission of argon atoms (a) and ions (b) in the axial region of an arc[13,14]: 1—total line intensity, 2—vertical polarization.

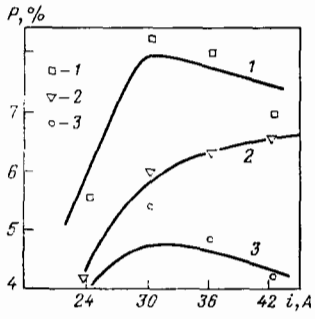

FIG. 23. Rotation of the plane of polarization of the line emission of an arc[13,14]: points—experimental, curves—calculated.

—independent determinations of $\rho^{(2)}/\rho^{(0)}$ for a particular state, using measurements of the polarization of two lines, yield very similar values

—the excited states of the ArII ion have values of $\rho^{(2)}/\rho^{(0)}$ that are higher by factors of 2–10 as compared with the states of the ArI atom

—the spatial distributions of degree of polarization shows that the polarization increases with increasing radial distance and with the rotation of the plane of polarization about the discharge axis through angles up to 45°.

This behavior of the polarization of radiation shows that it is due to the alignment of the observed excited states. Estimates of the contributions of possible alignment mechanisms show that the polarization is due to anisotropy in the motion of electrons.

The anisotropic properties of the electron distribution function under the conditions prevailing in the arc discharge at atmospheric pressure are examined theoretically in some detail in Ref. 42. The directed motion of electrons along the axis is due to the electric field of the arc current, whereas in the radial direction the motion is controlled by temperature gradients. The anisotropy in the motion of electrons is largely confined to electrons with energies $\gtrsim 10$ eV, which are responsible for the excitation of states and for their polarization. Thermal electrons with the isotropic distribution take part only in the relaxation of alignment. The dominant role of direct processes in establishing alignment, and the corresponding relationship (3.2) between the electron momentum flux tensor and the alignment tensor, are used to estimate the radial distribution of the rotation of the plane of polarization β for a number of ionic and atomic lines, and to compare the results with experimental data (Fig. 24). It is clear that the calculated curves are in good agreement with the experimental variation of β.

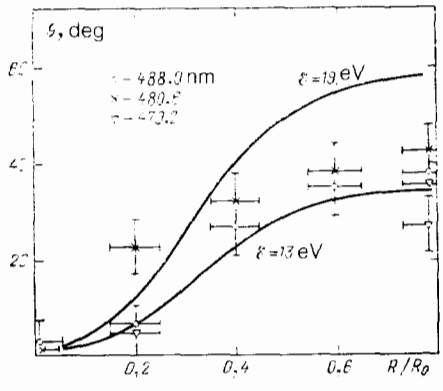

FIG. 24. Polarized emission by argon ions in the axial region of the plasma as a function of the arc current[13,14,42]: 1—488.0 nm, 2—480.6 nm, 3—454.5 nm; points—experimental, curves—calculated.

5.8. Chromospheric flares

Interest in the polarization of atomic ensembles has continued in astrophysics for nearly sixty years, ever since it was discovered that the emission of the solar corona was partially plane polarized. The polarization of the spectral lines was found to be due to the alignment of the excited states of particles absorbing resonance radiation from the interior of the solar atmosphere. Advances in quantitative studies of non-steady-state astrophysical processes capable of giving rise to instabilities and occasionally to catastrophes have resulted in an acute need for determinations of the spatial and angular distributions of the magnetic field vector and the velocities of different particles.[32] For example, measurements of the magnetic field and of the velocity field are necessary for the solution of the problem of the heating of the solar corona. Studies of acceleration mechanisms in the solar wind require knowledge of the magnetic field and the velocity field of radiating ions in the corona. Magnetic energy is converted in solar flares into kinetic energy by mechanisms that are not fully understood. Studies of energy transfer and of the transport modes require accurate knowledge of the velocity distribution of epithermal electrons. The polarization of atomic ensembles, which transforms information on vector quantities into observable Stokes parameters, can be used to investigate these and many other dynamic phenomena.

The polarization of spectral lines emitted by solar prominences[31,32] was extensively investigated in the 1960s and 1970s. The local magnetic field was estimated by assuming that the alignment of states was due to anisotropic optical excitation. The known geometry of the emission field, due to the spherical shape of the source of the emission, was then used together with additional information on the structure of the transition, the origin of the spectral lines, the parameters of the ambient medium, and the atomic constants, to calculate the polarization of the particle fluorescence in the absence of the magnetic field. Subsequent comparison between experimental data and the calculated values yielded the required magnetic field strength. Simultaneous observations of two or more spectral lines was then used to determine the direction of the magnetic field as well.

There have been relatively few polarization measurements of the particle velocity field in astrophysical objects, and further work in this area would be of considerable value.[32] Most of the existing results have been obtained by studying local formations in the solar atmosphere.[180,181] The problem has been to identify the mode of energy transfer from the interior to the chromospheric flares. Energy can be transferred by thermal conduction, by the dissipation of the energy of fast electron beams, and by irradiation with x rays. Studies of the relative contributions of these processes to the energy balance in chromospheric formations provide a basis for ideas on the global nature of solar flares.

Each of the above energy transfer channels should lead to a different local anisotropy in the motion of electrons in the region of a flare. The distribution function of electrons participating in the first two energy transfer mechanisms has a symmetry axis that points toward the center of the solar disk. Irradiation with x rays or the far ultraviolet gives rise to

an ensemble of photoelectrons with energies of the order of a few tens of eV (the energy of background electrons is of the order of a few eV) and to the preferential horizontal direction of motion.[182] Both groups of electrons can produce ensembles of excited particles for which the directions of the principal axes of alignment are determined by the directions of the symmetry axes of the corresponding EDFs. It follows that the measured Stokes parameters can be used to choose between different models of energy input, and even to estimate the amount of transferred energy.

The above researches have shown that the characteristic chromospheric lines of hydrogen and sulfur, emitted during solar flares, are partially plane polarized. The analyzer was the diffraction grating of a UV spectrometer, and the radiation was modulated by a rotating wave plate. Fourier analysis of the radiation intensity as a function of the rotation of the plate was then used to determine the Stokes parameters. Measurements on the H_α line[180,181] were performed over 4-min intervals corresponding to the decay of the two flares of 17 May 1980 (N 15, E 28) and 30 January 1981 (S 11, E 23). The mean polarization was found to be 2%. Figure 25 shows the polarization map for the SI sulfur line at 143.7 nm, recorded in bright portions of the flares during the decay phase on 15 July 1980 (S 218″, E 450″).[181] The polarization vector was also found to point toward the center of the solar disk, and the average polarization was of the order of 12%. Independent observations in the two chromospheric lines were thus found to yield similar results.

The polarization effects were interpreted as follows.[183] The first step was to isolate the principal energy transfer channel. Since, in all cases, the observations indicated a preferential radial orientation of the electric field relative to the solar disk, the effect of x-ray irradiation could be excluded. The other two channels were separated by using the dependence of the degree of polarization on the energy of exciting electrons. If it is assumed that the threshold polarization is positive, electrons with energies of 1–100 eV that participate in the thermal conduction process should also produce positive polarizations, whereas energetic beam electrons with energies of the order of a few keV should give rise to polarization of the opposite sign. These considerations and the experimental data led to conclusion that the principal channel for energy transfer to the chromospheric flares was thermal conduction by the electron gas.

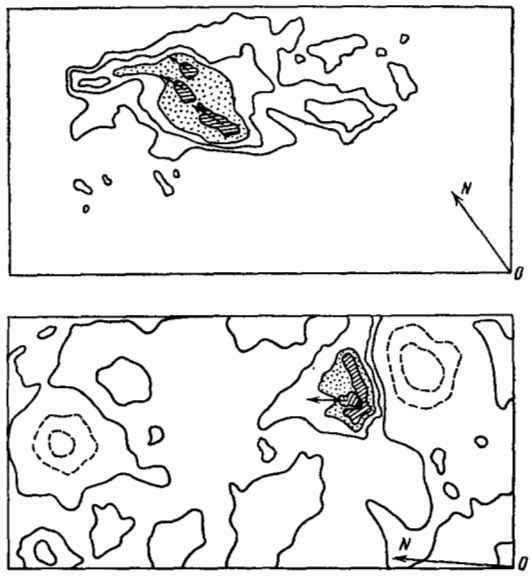

FIG. 25. Polarization map of the line emission of a chromospheric flare recorded in the sulfur line at 143.7 nm (Refs. 180 and 181).

Subsequent analysis based on a model distribution function for the electron gas[184] was used to estimate the relative heat flux to a flare, q/q_s ($q_s = 3N_e m_e v_T^3/2$). For the H_α line, it was found that $0.16 < q/q_s < 0.37$. For the 143.7-nm SI line, measurements showed that $0.13 < q/q_s < 0.33$, which is in good agreement with the results for H_α. Assuming that the electron density in this region was $\sim 10^{12}$ cm^{-3}, it was found that $q_s = 8\times 10^7$–2.3×10^8 erg/cm^2 s^{-1} (at temperatures in the range 10^4–2×10^4 K).[185] Thus, the authors of Refs. 184 and 185 were able, for the first time, to use polarization spectroscopy to obtain quantitative estimates for the energy balance in chromospheric formations. This showed that the energy transfer was of the order of the total radiative loss in the region of the flare, and of the same order or somewhat smaller than the heat transfer in the transition zone of the flare. These results demonstrated the importance of electrical conduction in the energy balance of chromospheric flares, and also the great usefulness of polarization spectroscopy in studies of astrophysical objects.

6. CONCLUSION

Polarization is an exceedingly powerful concept that can be exploited throughout science. In an ionized gas (plasma), it involves the collective effect of charge separation, the ability of atomic particles to acquire a dipole moment in an electric field, and the ordering of field orientations in the electromagnetic wave. Relatively recently it has become clear that another type of polarization, namely the polarization of ensembles of atomic particles, exists in plasmas. All these types of polarization are manifestations of departure from isotropy in the media under investigation. Their origin and existence must be due to common factors.

In plasmas, these common factors are the electric and magnetic fields, the potential gradients, the radiation and particle fluxes, the parameter gradients, and so on. These factors are also responsible for the very existence of the plasma. In fact, the fields control the energy input into the plasma, and confine it to a bounded volume. The properties of a plasma distinguish it sharply from the ambient medium, which then unavoidably gives rise to considerable potential gradients and discontinuities. The consequences of all this is *anisotropy* in the distribution of particles and radiation, which in turn gives rise to the polarization of the atomic ensemble.

It is legitimate to ask: how common is this type of polarization? We believe that the polarization of the atomic ensemble in a plasma is a rule rather than an exception, and that this is a phenomenon just as common as the collective effect of polarization due to charge separation. For example, the polarization of atomic ensembles was first discovered in low-pressure gas discharges. It was considered that it could not exist at higher-pressure plasmas because of collisional relaxation. The polarization of such ensembles was nevertheless detected under such conditions in the course of the last few years, and it was shown that there were fundamental

reasons that practically excluded the influence of collisional relaxation on the polarization of particle ensembles. The polarization was not readily detected because it had only indirect manifestations, namely, in the polarization of emission spectra.

The polarization spectrometry of plasmas, especially as applied to pulsed processes, has not been as widely used in experimental physics as it should. We hope that the extensive use of this technique will confirm our belief that the polarization phenomenon is universal. The connection between the different types of polarization that we have traced in this review and the utilization of the corresponding experimental techniques will become powerful tools for investigating the properties of plasmas and of plasma processes that are becoming increasingly important in modern science and technology.

It is our pleasant duty to thank V. N. Rebane for discussions and constructive criticisms.

[1)] Here and henceforth, unless otherwise indicated, the word *atom* will refer to a particle with atomic dimensions, i.e., an atom, ion, or molecule.

[2)] We note that the divergence of the expansion in terms of spherical harmonics implies, simply, that the motion of the high-energy electrons becomes beam-like.

[1]U. Fano, Phys. Rev. **90**, 577 (1953).
[2]U. Fano, Rev. Mod. Phys. **29**, 74 (1957).
[3]M. I. D'yakonov and V. I. Perel', Zh. Eksp. Teor. Fiz. **47**, 1483 (1964) [Sov. Phys. JETP **20**, 997 (1965)].
[4]W. Happer, Rev. Mod. Phys. **44**, 169 (1972).
[5]A. Omont, Atomic Physics, ed. by P. G. H. Sanders, Plenum Press, New York, London, 1971, p. 191.
[6]Y. Ohman, Mon. Not. R. Astron. Soc. **89**, 479 (1929).
[7]M. P. Chaĭka, Interference of Degenerate Atomic States [in Russian], Leningrad University Press, 1975.
[8]V. I. Perel' and I. V. Rogova, Zh. Eksp. Teor. Fiz. **65**, 1012 (1973) [Sov. Phys. JETP **38**, 501 (1974)].
[9]M. P. Chaĭka, Opt. Spektrosk. **30**, 822 (1971) [Opt. Spectrosc. (USSR) **30**, 443 (1971)].
[10]V. K. Prilipko and E. B. Aleksandrov, *ibid.* **55**, 560 (1983) [Opt. Spectrosc. (USSR) **55**, 331 (1983)].
[11]S. A. Kazantsev, Proc. Intern. Conf. on Plasma Physics, Göteborg, Sweden, 1982, p. 131; Pis'ma Zh. Eksp. Teor. Fiz. **37**, 131 (1983) [JETP Lett. **37**, 158 (1983)].
[12]S. A. Kazantsev and A. V. Subbotenko, Fiz. Plazmy **10**, 135 (1984) [Sov. J. Plasma Phys. **10**, 78 (1984)].
[13]L. Ya. Margolin, N. Ya. Polynovskaya, L. N. Pyatnitskiĭ, R. Sh. Timergaliev, and S. A. Edel'man, Sixth All-Union Conf. on Low-Temperature Plasma Physics. Abstracts of Papers [in Russian], Leningrad Institute of Nuclear Physics, 1983, Vol. 1, p. 58.
[14]L. Ya. Margolin, N. Ya. Polynovskaya, L. N. Pyatnitskii, R. Sh. Timergaliev, and S. A. Edel'man, Teplofiz. Vys. Temp. **23**, 193 (1984) [High Temp. (USSR) **22**, 149 (1984)].
[15]V. N. Rebane, Opt. Spektrosk. **24**, 309 (1968) [Opt. Spectrosc. (USSR) **24**, 163 (1968)].
[16]A. G. Petrashen', V. N. Rebane, and T. K. Rebane, Zh. Eksp. Teor. Fiz. **87**, 147 (1984) [Sov. Phys. JETP **60**, 84 (1984)].
[17]A. G. Petrashen', V. N. Rebane, and T. K. Rebane, Opt. Spektrosk. **58**, 785 (1985) [Opt. Spectrosc. (USSR) **58**, 481 (1985)].
[18]S. A. Kazantsev, N. T. Polezhaeva, A. G. Petrashen', V. N. Rebane, and T. K. Rebane, Pis'ma Zh. Eksp. Teor. Fiz. **45**, 15 (1987) [JETP Lett. **45**, 17 (1987)].
[19]U. Fano, Phys. Rev. B **133**, 828 (1964).
[20]M. Lombardi, J. Phys. (Paris) **30**, 631 (1969).
[21]A. G. Petrashen', V. N. Rebane, and T. K. Rebane, Opt. Spektrosk. **61**, 214 (1986) [Opt. Spectrosc. (USSR) **61**, 138 (1986)].
[22]W. Hanle, Z. Phys. **30**, 93 (1924).
[23]R. M. Imhof and F. H. Reed, Rep. Prog. Phys. **40**, 1 (1977).
[24]M. I. D'yakonov and V. I. Perel', Zh. Eksp. Teor. Fiz. **48**, 345 (1965) [Sov. Phys. JETP **21**, 227 (1965)].
[25]M. I. D'yakonov, Zh. Eksp. Teor. Fiz. **47**, 2213 (1964) [Sov. Phys. JETP **20**, 1484 (1965)].
[26]B. Budick, Advances in Atomic and Molecular Physics, ed. by D. R. Bates and E. I. Esterman, Academic Press, N. Y., 1967, Vol. 3, p. 48.
[27]S. P. Dmitriev, G. A. Zhitnikov, and A. I. Okunevich, see Ref. 13, Vol. 2, p. 112.
[28]S. G. Rautian, G. I. Smirnov, and A. M. Shalagin, Nonlinear Resonances in the Spectra of Atoms and Molecules [in Russian], Nauka, Novosibirsk, 1979.
[29]H. W. B. Skinner, Proc. R. Soc. London **112**, 642 (1926).
[30]D. A. Varshalovich, Usp. Fiz. Nauk **101**, 369 (1970) [Sov. Phys. Usp. **13**, 429 (1971)].
[31]S. A. Kazantsev, Usp. Fiz. Nauk **139**, 621 (1983) [Sov. Phys. Usp. **26**, 328 (1983)].
[32]S. Sahal-Brechot, Ann. Phys. (Paris) **9**, 705 (1984).
[33]Kh. V. Kallas and M. P. Chaĭka, Opt. Spektrosk. **27**, 694 (1969) [Opt. Spectrosc. (USSR) **27**, 376 (1969)].
[34]C. G. Carrington and A. Corney, Opt. Commun. **1**, 115 (1969).
[35]M. Lombardi and J. C. Pebay-Peyroula, C. R. Acad. Sci. Ser. B **261**, 1485 (1965).
[36]V. N. Grigor'eva, S. A. Kazantsev, M. A. Kudryasheva, *et al.*, Opt. Spektrosk. **54**, 421 (1983) [Opt. Spektrosc. (USSR) **54**, 247 (1983)].
[37]E. P. Busygin, S. I. Vlasenko, V. G. Grigor'yants, and V. P. Popovich, Zh. Tekh. Fiz. **47**, 1889 (1977) [Sov. Phys. Tech. Phys. **22**, 1095 (1977)].
[38]V. G. Borodin and Yu. M. Kagan, Opt. Spektrosk. **18**, 966 (1965) [Opt. Spectrosc. (USSR) **18**, 546 (1965)].
[39]D. Z. Zhechev, S. A. Kazantsev, and M. P. Chaĭka, Proc. Seventh National Conf. on Spectroscopy, Bulgaria [in Russian], 1976, p. A11.
[40]E. P. Busygin and V. G. Grigor'yants, Zh. Tekh. Fiz. **46**, 2362 (1976) [Sov. Phys. Tech. Phys. **21**, 1390 (1976)].
[41]E. P. Bysygin, V. G. Grigor'yants, and I. P. Yavor, Zh. Tekh. Fiz. **47**, 1190 (1977) [Sov. Phys. Tech. Phys. **22**, 684 (1977)].
[42]S. Ya. Bronin, L. Ya. Margolin, N. Ya. Polynovskaya, L. N. Pyatnitskiĭ, and S. A. Edel'man, Preprint Institute of High Temperatures, USSR Academy of Sciences No. 5-129 [in Russian], M., 1984.
[43]A. S. Antonov, V. M. Batenin, A. T. Kunavin, N. Ya. Polynovskaya, L. N. Pyatnitskiĭ, and S. A. Edel'man, Preprint Institute of High Temperatures, USSR Academy of Sciences No. 6-130 [in Russian], M., 1984.
[44]L. Ya. Margolin, N. Ya. Polynovskaya, L. N. Pyatnitskiĭ, R. Sh. Timirgaliev, and S. A. Edel'man, Tech. Information No. 81016983 [in Russian], Institute of High Temperatures, USSR Academy of Sciences, M., 1982.
[45]R. A. Duncan, Planetary and Space Science, Pergamon Press, N. Y., 1959, Vol. 1, p. 112.
[46]L. D. Landau and E. M. Lifshitz, Quantum Mechanics: Nonrelativistic Theory, Pergamon Press, Oxford, 3rd Ed., 1977 [Russ. original, Nauka, M., 1974].
[47]K. Blum, Density Matrix Theory and Applications, Plenum Press, N. Y., 1981 [Russ. transl. Mir, M., 1986].
[48]J. P. Elliott and P. G. Dawber, Symmetry in Physics, McMilian, London, 1979 [Russ. transl. of previous ed., Mir, M., 1974].
[49]L. D. Landau and E. M. Lifshitz, The Classical Theory of Fields, 4th ed., Pergamon Press, Oxford, 1975 [Russ. original, Nauka, M., 1973].
[50]A. Abragam, The Principles of Nuclear Magnetism, Clarendon Press, Oxford, 1961 [Russ. transl., IL, M., 1963].
[51]M. I. D'yakonov and V. I. Perel', Opt. Spektrosk. **20**, 472 (1968) [Opt. Spectrosc. (USSR) **20**, 257 (1968)].
[52]C. Cohen-Tannoudji, Ann. Phys. (Paris) **7**, 423 (1962).
[53]B. Decomps, M. Dumont, and M. Ducloy, in Laser Spectroscopy of Atoms and Molecules, ed. by H. Walther, Springer-Verlag, Berlin, 1976, pp. 284-347 [Russ. transl. Mir, M., 1979].
[54]I. Hertel and W. Stoll, Adv. Atom. Mol. Phys. **13**, 113 (1977).
[55]D. A. Varshalovich, A. N. Moskalev, and V. K. Khersonskiĭ, Quantum Theory of Angular Momentum [in Russian], Nauka, L., 1975.
[56]V. N. Rebane, T. K. Rebane, and A. I. Sherstyuk, Opt. Spektrosk. **51**, 753 (1981) [Opt. Spektrosc. (USSR) **51**, 418 (1981)].
[57]M. Ducloy, Ann. Phys. (Paris) **8**, 403 (1973-1974).
[58]V. N. Rebane, Abstract of Doctoral Thesis-Phys. Math. Sci. [in Russian], Leningrad University, 1980.
[59]A. Omont, Prog. Quantum Electron. **5**, 69 (1977).
[60]E. B. Aleksandrov and M. P. Chaĭka, Izv. Akad. Nauk SSSR Ser. Fiz. **48**, 633 (1984) [Bull. Acad. Sci. USSR Phys. Ser. 48 (4), 8 (1984)].
[61]M. P. Chaĭka, Avtometriya No. 1, 104 (1979).
[62]O. Nedelec, J. Phys. (Paris) **27**, 660 (1966).
[63]I. C. Persival and M. J. Seaton, Proc. Phys. Soc. London **53**, 68 (1957).
[64]I. I. Sobel'man, Introduction to the Theory of Atomic Spectra, Pergamon Press, Oxford, 1972 [Russ. original, Nauka, M., 1977].
[65]J. Macek, Electron and Photon Interactions with Atoms, Academic Press, N. Y., 1976.
[66]I. V. Hertel and K. J. Ross, Phys. Rev. Lett. **21**, 1511 (1968).
[67]J. Macek and I. V. Hertel, J. Phys. B **7**, 2173 (1974).

[68]S. A. Kazantsev and A. G. Rys', Abstracts of Papers presented at the Second All-Union Conf. on Quantum Metrology and Fundamental Physical Constants [in Russian], Leningrad, 1985, p. 137.
[69]U. Fano and J. Macek, Rev. Mod. Phys. **45**, 553 (1973).
[70]M. Matsuzawa, H. Mitsuoka, and M. Inokuti, J. Phys. B **12**, 3033 (1979).
[71]S. C. McFarlane, *ibid.* 7, 1756 (1974).
[72]B. H. Brandsen and M. C. R. McDowell, Phys. Rep. **46**, 243 (1978).
[73]H. Kleinpoppen and A. Scharmann, Progress in Atomic Spectroscopy, Plenum Press, P. A.-N. Y., 1979.
[74]A. G. Petrashen', V. N. Rebane, and T. K. Rebane, Opt. Spektrosk. **57**, 200 (1984) [Opt. Spectrosc. (USSR) **57**, 122 (1984)].
[75]A. G. Petrashen', V. N. Rebane, and T. K. Rebane, *ibid.* **58**, 983 (1985) [Opt. Spectrosc. **58**, 598 (1985)].
[76]E. Chamoun, M. Lombardi, M. Carre, and M. L. Gaillard, J. Phys. (Paris) **38**, 581 (1977).
[77]E. N. Kotlikov and M. P. Chaĭka, Opt. Spektrosk. **55**, 242 (1983) [Opt. Spectrosc. (USSR) **55**, 142 (1983)].
[78]T. Manabe, T. Yabuzaki, and T. Ogawa, Phys. Rev. Lett. **46**, 637 (1981).
[79]T. Manabe, T. Yabuzaki, and T. Ogawa, Phys. Rev. A **20**, 1946 (1979).
[80]L. M. Biberman, V. S. Vorob'ev, and I. T. Yakubov, Kinetics of Nonequilibrium Low-Temperature Plasmas, Consultants Bureau, N. Y., 1987 [Russ. original Nauka, M., 1982].
[81]N. L. Aleksandrov, A. M. Konchakov, A. P. Napartovich, and A. N. Starostin, Plasma Chemistry [in Russian], ed. by B. M. Smirnov, Energoatomizdat, M., 1984, No. 11, p. 3.
[82]L. C. Pitchford, S. V. O'Neil, and J. R. Rumbl Jr., Phys Rev. A **23**, 294 (1981).
[83]L. C. Pitchford and A. V. Phelps, *ibid.* **25**, 540 (1982).
[84]P. Segur, M. C. Bordage, J. P. Balagner, and M. Yousbj, J. Comput. Phys. **50**, 116 (1983).
[85]S. L. Lin, R. E. Robsoson, and E. A. Mason, J. Chem. Phys. **71**, 3483 (1979).
[86]H. Tagashira, Y. Sakai, and S. Sacamoto, J. Phys. D **10**, 1051 (1977).
[87]A. V. Phelps and L. C. Pitchford, Phys. Rev. A **31**, 2932 (1985).
[88]H. A. Blevin, J. Fletcher, and S. R. Hunter, *ibid.* 2215.
[89]G. N. Haddat, S. K. Lin, and R. E. Robson, Aust. J. Phys. **34**, 243 (1981).
[90]V. L. Ginzburg and A. V. Gurevich, Usp. Fiz. Nauk **70**, 201 (1960) [Sov. Phys. Usp. **3**, 115 (1960)].
[91]S. A. Kazantsev, N. Ya. Polynovskaya, L. N. Pyatnitskiĭ, and S. A. Edel'man, Opt. Spektrosk. **58**, 48 (1985) [Opt. Spectrosc. **58**, 28 (1985)].
[92]S. A. Kazantsev and A. V. Subbotenko, *ibid.* **60**, 257 (1986) [Opt. Spectrosc. (USSR) **60**, 157 (1986)].
[93]I. D. Reid, Aust. J. Phys. **32**, 231 (1979).
[94]I. D. Reid and S. R. Hunter, *ibid.* **32**, 255.
[95]J. P. Bromberg, J. Chem. Phys. **50**, 3906 (1969).
[96]T. G. Finn and T. P. Doering, *ibid.* **63**, 4399 (1975).
[97]S. K. Srivastava, A. Shutjian, and S. Trajmar, *ibid.* **64**, 1340 (1976).
[98]T. W. Shyn and G. R. Carignan, Phys. Rev. A **22**, 923 (1980).
[99]M. E. Riley, C. J. MacCalium, and F. Biggs, At. Data and Nuclear Data Tabl. **15**, 443 (1975).
[100]A. B. Alexandrov and M. P. Chaĭka, Sov. Sci. Rev. Ser. A: Phys. Rev. **6**, 1, 1985.
[101]P. M. Doherty and D. R. Crosley, Appl. Opt. **23**, 713 (1984).
[102]J. P. Barrat, M. D. Casalta, J. L. Cojan, and J. Hamel, J. Phys. (Paris) **27**, 608 (1966).
[103]N. G. Preobrazhenskiĭ and V. P. Pikalov, Instability Problems in Plasma Diagnostics [in Russian], Nauka, Novosibirsk, 1982.
[104]P. S. Hauge, Surface Sci. **96**, 108 (1980).
[105]P. S. Hauge, R. H. Muller, and C. C. Smith, *ibid.* 81.
[106]V. S. Zapasskii, Zh. Prikl. Spektrosk. **37**, 181 (1982) [J. Appl. Spectrosc. (USSR) **37**, 857 (1982)].
[107]G. G. Dolgov, Opt. Spektrosk. **6**, 717 (1959) [Opt. Spectrosc. (USSR) **6**, 469 (1959)].
[108]G. Markova and M. Chaĭka, *ibid.* **17**, 319 (1964) [Opt. Spectrosc. (USSR) **17**, 170 (1964)].
[109]V. A. Dombrovskiĭ, Astron. Zh. **30**, 319 (1953).
[110]S. E. Pellicori and R. R. Gray, Appl. Opt. **6**, 1121 (1967).
[111]J. C. Henoux *et al.*, Astron. J. **265**, 1066 (1983).
[112]E. P. Busygin, V. G. Grigor'yants, and N. I. Yavor, Zh. Prikl. Spektrosk. **18**, 1100 (1973) [J. Appl. Spectrosc. (USSR) **18**, 807 (1973)].
[113]L. R. Danielsson and G. H. Kasai, Geophys. Res. **73**, 259 (1968).
[114]L. Danielsson, Phys. Fluids **13**, 2288 (1970).
[115]S. A. Kazantsev and A. V. Subbotenko, Opt. Spektrosk. **55**, 767 (1983) [Opt. Spectrosc. (USSR) **55**, 458 (1983)].
[116]R. M. Azzam and N. M. Bashara, Ellipsometry and Polarized Light, Elsevier, N. Y., 1977 [Russ. transl., Mir, M., 1981].
[117]V. V. Beloshitskiĭ, A. A. Kuts, L. Ya. Margolin, L. N. Pyatnitskiĭ, A. I. Romashevskiĭ, and S. A. Edel'man, Preprint Institute of High Temperatures, USSR Academy of Sciences, No. 5-153 [in Russian], M., 1985.
[118]W. Happer, Beam-Foil Spectroscopy, ed. by S. Bashkin, Academic Press, N. Y.-London, 1968.
[119]L. Ya. Novikov, G. V. Sirotskiĭ, and G. I. Solomakho, Usp. Fiz. Nauk **113**, 398 (1974) [Sov. Phys. Usp. **17**, 815 (1975)].
[120]S. A. Kazantsev and A. G. Rys', Abstracts of Papers presented at the All-Union Conf. on Optical Orientation of Atoms and Molecules [in Russian], Leningrad, 1986, p. 64.
[121]V. I. Babanin, L. A. Bakaleĭnikov, E. P. Busygin, V. G. Grigor'yants, and A. Ya. Ender, Zh. Tekh. Fiz. **49**, 2596 (1979) [Sov. Phys. Tech. Phys. **23**, 1487 (1979)].
[122]A. Z. Dolginov, Yu. N. Gnedin, and N. A. Silant'ev, Propagation and Polarization of Radiation in Cosmic Medium [in Russian], Nauka, M., 1979.
[123]S. A. Kazantsev, L. Ya. Margolin, N. Ya. Polynovskaya, L. N. Pyatnitskiĭ, and S. A. Edel'man, Opt. Spektrosk. **55**, 553 (1983) [Opt. Spectrosc. (USSR) **55**, 326 (1983)].
[124]S. A. Kazantsev, A. Kisling, and M. P. Chaĭka, *ibid.* **34**, 1227 (1973) [Opt. Spectrosc. (USSR) **34**, 714 (1973)].
[125]L. M. Volkova, A. M. Devyatov, and E. A. Kral'kina, Ill-Posed Inverse Problems in Atomic Physics [in Russian], Institute of Theoretical and Applied Mechanics, Siberian Branch of the Academy of Sciences of the USSR, Novosibirsk, 1976.
[126]V. I. Krylov and N. S. Skoblya, Approximate Laplace Transform Method [in Russian], Nauka, M., 1974.
[127]K. Blum and H. Kleinpoppen, Phys. Rep. **52**, 203 (1979).
[128]N. Ya. Polynovskaya, Abstracts of Papers presented at the Ninth All-Union Conf. on the Physics of Electron-Atom Collisions [in Russian], Institute of Physics, Academy of Sciences of the Latvian SSR, Riga, 1984, Vol. 2, p. 48.
[129]M. Inokuti, Rev. Mod. Phys. **43**, 297 (1971).
[130]B. H. Bransden and M. C. R. McDowell, Phys. Rep. C **30**, 206 (1977).
[131]A. Chutjian and D. C. Cartwright, Phys. Rev. A **23**, 2178 (1981).
[132]L. D. Tsendin and Yu. B. Golubovskiĭ, Zh. Tekh. Fiz. **47**, 1839 (1977) [Sov. Phys. Tech. Phys. **22**, 1066 (1977)].
[133]L. D. Tsendin, Zh. Tekh. Fiz. **48**, 1569 (1978) [Sov. Phys. Tech. Phys. **23**, 890 (1978)].
[134]C. G. Carrington and A. Corney, J. Phys. B **4**, 849 (1971).
[135]C. G. Carrington, A. Corney, and A. V. Durrant, *ibid.* **5**, 1001 (1972).
[136]S. A. Kazantsev, A. Kisling, and M. P. Chaĭka, Opt. Spektrosk. **36**, 1030 (1974) [Opt. Spectrosc. (USSR) **36**, 605 (1974)].
[137]J. P. Grandin, D. Lecleur, and J. Mergerie, J. Phys. (Paris) **34**, 403 (1973).
[138]S. A. Kazantsev, A. Kisling, V. N. Markov, and M. P. Chaĭka, Vestn. Leningr. Univ. Fiz. Khim. No. **10**, 33 (1975).
[139]X. Husson and J. P. Grandin, J. Phys. (Paris) **39**, 933 (1978).
[140]J. P. Lemoique, X. Husson, and J. Margerie, Opt. Commun. **15**, 241 (1975).
[141]S. A. Kazantsev, A. G. Rys', and M. P. Chaĭka, Opt. Spektrosk. **44**, 425 (1978) [Opt. Spectrosc. **44**, 249 (1978)].
[142]X. Husson and J. Margerie, Opt. Commun. **5**, 139 (1972)].
[143]S. A. Kazantsev, V. P. Markov, S. A. Morozova, and M. P. Chaĭka, Opt. Spektrosk. **46**, 1096 (1979) [Opt. Spectrosc. (USSR) **46**, 619 (1979)].
[144]C. G. Carrington, J. Phys. B **5**, 1572 (1972).
[145]S. A. Kazantsev, Vestn. Leningr. Univ. Fiz. Khim. No. 4, 52 (1980).
[146]S. A. Kazantsev, A. G. Rys', and M. P. Chaĭka, Opt. Spektrosk. **54**, 214 (1983) [Opt. Spectrosc. (USSR) **54**, 124 (1983)].
[147]Yu. P. Raĭzer, Fiz. Plazmy **5**, 408 (1979) [Sov. J. Plasma Phys. **5**, 232 (1979)].
[148]S. M. Levitskiĭ, Zh. Tekh. Fiz. **27**, 1001 (1957) [Sov. Phys. Tech. Phys. **2**, 913 (1958)].
[149]V. A. Godyak, A. A. Kuzovinkov, V. P. Savinov, *et al.*, Vestn. Mosk. Univ. Fiz. Astron. No. 2, 126 (1968).
[150]A. A. Kuzovnikov and V. P. Savinov, Problems in Low-Temperature Plasma Physics [in Russian], Minsk, 1970.
[151]A. A. Kuzovnikov and V. P. Savinov, Radiotekh. Elektron. **18**, 816 (1973) [Radio Eng. Electron. Phys. (USSR) **18**, 593 (1973)].
[152]A. A. Kuzovnikov and V. P. Savinov, Vestn. Mosk. Univ. Fiz. Astron. No. 2, 215 (1973).
[153]S. A. Kazantsev, A. E. Svelokurov, and A. V. Subbotenko, Zh. Tekh. Fiz. **56**, 1091 (1986) [Sov. Phys. Tech. Phys. **31**, 638 (1986)].
[154]V. A. Godyak and A. Kh. Ganna, Fiz. Plazmy **6**, 676 (1980) [Sov. J. Plasma Phys. **6**, 372 (1980)].
[155]V. A. Godyak, Zh. Tekh. Fiz. **41**, 1364 (1971) [Sov. Phys. Tech. Phys. **16**, 1073 (1972)].
[156]S. A. Kazantsev and A. V. Subbotenko, Pis'ma Zh. Tekh. Fiz. **10**, 1251 (1984) [Sov. Tech. Phys. Lett. **10**, 529 (1984)].
[157]L. Danielsson and L. Lindberg, J. Phys. E **7**, 817 (1974).

[158]L. Danielsson and L. Lindberg; Trans. R. Inst. Techn. Stockholm **17**, 1 (1979).
[159]H. Alfven, On the Origin of the Solar System, Oxford University Press, 1964.
[160]R. H. McFarland and E. A. Soltysie, Phys. Rev. **127**, 2090 (1962).
[161]H. H. Moustafa Moussa, E. J. de Heer, and J. Shutten, Physica (Utrecht) **40**, 517 (1969).
[162]Yu. A. Byrdin, B. Ya. Lyubimov, and A. F. Nastoyashchiĭ, Teplofiz. Vys. Temp. **5**, 25 (1967) [High Temp. (USSR) **5**, 21 (1967)].
[163]G. A. Dyuzhev, B. Ya. Moizhes, E. A. Startsev, *et al.*, Zh. Tekh. Fiz. **41**, 2393 (1971) [Sov. Phys. Tech. Phys. **16**, 1900 (1971)].
[164]G. A. Dyuzhev, B. Ya. Moizhes, V. A. Nemchinskiĭ, *et al.*, Zh. Tekh. Fiz. **41**, 2406 (1971) [Sov. Phys. Tech. Phys. **16**, 1910 (1971)].
[165]J. C. Gay and W. B. Schneider, J. Phys. (Paris) **36**, L239 (1975).
[166]J. C. Gay, *ibid.* L239.
[167]V. P. Popovich, T. A. Nevskova, I. F. Kharchenko, and E. G. Shustin, Izv. Vyssh. Uchebn. Zaved. Radiofiz. **16**, 1709 (1973) [Radiophys. Quantum Electron. **16**, 854 (1973)].
[168]I. F. Kharchenko, Ya. B. Faĭnberg, R. M. Nikolaev, E. A. Kornilov, *et al.* Zh. Tekh. Fiz. **31**, 761 (1961) [Sov. Phys. Tech. Phys. **6**, 551 (1961)].
[169]A. I. Akhiezer and Ya. B. Faĭnberg, Dokl. Akad. Nauk SSSR **69**, 555 (1949).
[170]H. A. Boot, S. A. Self, and R. B. Q. Shersby, J. Electron. Control **4**, 434 (1958).
[171]G. A. Askar'yan, At. Energ. **4**, 71 (1958).
[172]E. A. Abramyan, B. A. Al'terkop, and G. D. Kuleshov, Preprint, Institute of High Temperatures of the USSR Academy of Sciences No. 6-092 [in Russian], M., 1982.
[173]Main results of Scientific Research at the Institute of High Temperatures of the USSR Academy of Sciences in 1980 [in Russian], Nauka, M., 1981, p. 95.
[174]A. A. Rukhadze, L. S. Bogdankevich, S. E. Rosinskiĭ, and V. G. Rukhlin, Physics of High-Current Relativistic Electron Beams [in Russian], Atomizdat, M., 1980.
[175]L. M. Anosova and L. M. Gorbunov, Zh. Tekh. Fiz. **47**, 1150 (1977) [Sov. Phys. Tech. Phys. **22**, 660 (1977)].
[176]E. S. Bandaletova, V. M. Batenin, S. V. Lyuzin, and P. V. Minaev, Proc. Sixth All-Union Conf. on Low-Temperature Plasma Sources [in Russian], Ilim, Frunze, 1974, p. 373.
[177]V. M. Batenin, L. Ya. Margolin, and L. N. Pyatnitskiĭ, Fiz. Plazmy **5**, 517 (1979) [Sov. J. Plasma Phys. **5**, 285 (1979)].
[178]L. Ya. Margolin, Author's Abstract of Thesis for Candidate of Phys. Math. Sciences [in Russian], Institute of High Temperatures, Academy of Sciences of the USSR, M., 1978.
[179]V. M. Batenin and P. V. Minaev, Teplofiz. Vys. Temp. **9**, 676 (1971) [High Temp. (USSR) **9**, 619 (1971)].
[180]J. C. Henoux, M. Semel, G. Chambe, *et al.*, Astron. J. **265**, 1066 (1983).
[181]J. C. Henoux and M. Semel, The Year of the Solar Maximum [in Russian], Institute of Terrestrial Magnetism, the Ionosphere, and Radio Wave Propagation, USSR Academy of Sciences, M., 1981, Vol. 1, p. 201.
[182]G. Chambe and J. C. Henoux, Astron. Astrophys. **80**, 123 (1979).
[183]J. C. Henoux, D. Heristchi, G. Chambe, *et al.*, *ibid.* **119**, 233 (1983).
[184]W. M. Manheimer, Phys. Fluids **20**, 265 (1977).
[185]M. E. Machado, E. M. Avrett, J. E. Vernzza, *et al.*, Astrophys. J. **242**, 336 (1980).
[186]S. A. Kazantsev, N. T. Polezhaeva, and V. N. Rebane, Opt. Spektrosk. **63**, 27 (1987) [Opt. Spectrosc. (USSR) **63**, 15 (1987)].
[187]S. A. Kazantsev, A. G. Petrashen, N. T. Polezhaeva, V. N. Rebane, and T. K. Rebane, Europhys. Conf. Abstracts **11E**, C3-12 (1987).
[188]S. A. Kazantsev, Opt. Spektrosk. **52**, 931 (1982) [Opt. Spectrosc. (USSR) **52**, 559 (1982)].
[189]S. A. Kazantsev and A. V. Subbotenko, J. Phys. D **20**, 741 (1987).
[190]S. A. Kazantsev and A. V. Subbotenko, Vestn. Leningr. Univ. Fiz. Khim. No. 25, 20 (1987).
[191]S. A. Kazantsev, A. G. Rys', and A. V. Subbotenko, Fiz. Plazmy **14**, 215 (1988) [Sov. J. Plasma Phys.
[192]A. I. Drachev, S. A. Kazantsev, A. G. Rys', and A. V. Subbotenko, Opt. Spektrosk. **64**, 725 (1988) [Opt. Spectrosc. (USSR).
[193]S. A. Kazantsev and V. P. Markov, *ibid.* **36**, 613 (1974) [Opt. Spectrosc. (USSR) **36**, 355 (1974)].
[194]S. A. Kazantsev and E. S. Polzik, *ibid.* **41**, 1092 (1976) [Opt. Spectrosc. (USSR) **41**, 645 (1976)].
[195]S. A. Kazantsev and A. G. Rys', *ibid.* **43**, 575 (1977) [Opt. Spectrosc. (USSR) **43**, 339 (1977)].
[196]S. A. Kazantsev and V. I. Eĭduk, *ibid.* **45**, 858 (1978) [Opt. Spectrosc. (USSR) **45**, 735 (1978)].
[197]S. A. Kazantsev and V. P. Markov, *ibid.* **47**, 197 (1979) [Opt. Spectrosc. (USSR) **47**, 112 (1979)].
[198]S. A. Kazantsev and A. V. Subbotenko, *ibid.* **55**, 767 (1983) [Opt. Spectrosc. (USSR) **55**, 458 (1983)].
[199]S. A. Kazantsev, O. V. Smirnov, and A. V. Subbotenko, Vestn. Leningr. Univ. Fiz. Khim. No. **18**, 12 (1988).

Translated by S. Chomet